Improvement of Seaworthiness of Fast Catamaran by Hydrofoils Support

Camilo Mejía Jaramillo

Master Thesis

presented in partial fulfillment
of the requirements for the double degree:
“Advanced Master in Naval Architecture” conferred by University of Liege
"Master of Sciences in Applied Mechanics, specialization in Hydrodynamics, Energetics and Propulsion” conferred by Ecole Centrale de Nantes

developed at University of Rostock
in the framework of the

“EMSHIP”
Erasmus Mundus Master Course
in “Integrated Advanced Ship Design”

Ref. 159652-1-2009-1-BE-ERA MUNDUS-EMMC

Supervisor: Prof. Nikolai Kornev, University of Rostock

Reviewer: Prof. Florin Pacuraru, University of Galati

Rostock, February 2017

ABSTRACT

Improvement of seaworthiness of fast catamarans by hydrofoils support

By **Camilo Mejía Jaramillo**

The multihull vessels provide better stability, seakeeping and performance conditions than mono-hull crafts, this is one of the reasons whereby during the last 33 years the fast catamarans, able to reach 30 to 50 knots or more, have been used widely in important naval applications such as short- middle distance passenger fast ferry transport and offshore operational support, like oil platform and wind turbine farms.

Even with their good ones operational conditions the fast catamarans have limitations, as insufficient seakeeping qualities in rough seas, specially at high accelerations in head and oblique waves, mostly due to the slender hull shape that they use. The fast ferry transport and the offshore operational support normally take place, where the sea conditions are unsteady, to navigate through the irregular and multidirectional waves implies, among others, the increasing of the slamming force effects, higher amplitudes in the heave and pitch movements of the ship, major vertical accelerations at LCG and bow, vibrations and wave added resistance also.

The above situations produce uncomfortable rides, longer duration of the travels because low velocity operations, higher fuel consumption, lower safety levels, more engine power request, drag rising and electrical device damages, which increases the costs. Go as faster, economical and comfortable as possible always have been an imperative factor for passenger ferry transport and offshore operational support activities, for those reasons multiple options have been tested along the years in order to overcome the difficulties, already expressed, of sailing across adverse sea states.

The aim of this work is to show the benefits that the hydrofoils have to damp the longitudinal oscillation in rough seas, increase performance to the decrease the frictional drag in calm water and how it can be worth economically for catamarans supporting vessels. The foils exert a force in the hull upwards, moving it up, this event produce a vertical acceleration reduction due to the lower amplitude motion response reached at heave and pitch and the minor wetted area exposed to have the hull in a higher position from the undisturbed free surface level.

A non linear time domain mathematical model have been implemented, using C++ programming language, the model is based on the Zarnick´s method to predict vertical motions of a planing hull in regular and head waves, it was extended to incorporate the influence of the hydrofoils in the movements in order to perform comparisons among a single fast hull and hydrofoil configuration.

As it was predicted the results were satisfactory making evident the advantages that the hydrofoils have to improve seakeeping, worth noting that at higher wave amplitudes and wavelengths a fixed hydrofoil arrangement has a trend to follow the wave movement, therefore a lift control device is required to achieve the longitudinal damp expected.

From economical point of view the hydrofoil allows the ship navigate more time under rough seas, enhancing the rides comfort, saving money, now an analysis between the amount saved and the cost of installing, operation and maintenance takes place.

TABLE OF CONTENTS

Declaration of Authorship

I declare that this thesis and the work presented in it are my own and have been generated by me as the result of my own original research.

Where I have consulted the published work of others, this is always clearly attributed.

Where I have quoted from the work of others, the source is always given. With the exception of such quotations, this thesis is entirely my own work.

I have acknowledged all main sources of help.

Where the thesis is based on work done by myself jointly with others, I have made clear exactly what was done by others and what I have contributed myself.

This thesis contains no material that has been submitted previously, in whole or in part, for the award of any other academic degree or diploma.

I cede copyright of the thesis in favour of the University of Rostock

Date: *Signature*

"To my family, who is the engine of my life"

NOMENCLATURE

aBF = Buoyancy correction factor

aBM = Moment correction factor

b = Half beam

B = Beam of the hull, B = 2b

Cv = Beam Froude number

C∆ = Load coefficient

CD = Cross flow drag coefficient

d = Depth of penetration of each section

D = Friction drag

E = Wave slope

Fz = Hydrodynamic force in z direction

Fθ = Hydrodynamic moment about pitch axis

g = Acceleration due to gravity

I = Pitch moment of inertia

Ia = Added pitch moment of inertia

k = Wave number

ka = Added mass coefficient

lpp = Length of the hull

LCG = *Longitudinal centre of gravity*

ma = Sectional added mass

M = Mass of planing craft

Ma = Added mass of planing craft

N = Hydrodynamic normal force

U = Craft velocity parallel to keel

V = Craft velocity perpendicular to keel

VCG = *Vertical centre of gravity*

W = Weight of craft

wz = Wave orbital velocity in vertical direction

xc = Distance from centre of gravity to centre of pressure for normal force

xd = Distance from centre of gravity to centre of action for friction drag

xp = Moment arm of thrust about centre of gravity

xCG ẋCG ,ẍCG = Surge displacement, velocity and acceleration

zCG żCG ,zCG = Heave displacement, velocity and acceleration

θ,θ,θ = Pitch angle, velocity and acceleration

η = Wave elevation

η_0 = *Wave amplitude*

β = Deadrise angle

λ = Wave length

ω = Wave frequency

ρ = Density of water

1. INTRODUCTION

The multihull vessels provide better stability, seakeeping and performance conditions than mono-hull crafts[8], this is one of the reasons whereby during the last 33 years the fast catamarans, able to reach 30 to 50 knots or more, have been used widely in important naval applications such as short- middle distance passenger fast ferry transport[3] and offshore operational support, like oil platform and wind turbine farms.

Even with their good ones operational conditions the fast catamarans have limitations, as insufficient seakeeping qualities in rough seas, specially at high accelerations in head and oblique waves, mostly due to the slender hull shape that they use[3]. The fast ferry transport and the offshore operational support normally take place, where the sea conditions are unsteady, to navigate through the irregular and multidirectional waves implies, among others, the increasing of the slamming force effects, higher amplitudes in the heave and pitch movements of the ship, major vertical accelerations at LCG and bow, vibrations and wave added resistance also.

The above situations produce uncomfortable rides, longer duration of the travels because low velocity operations, higher fuel consumption, lower safety levels, more engine power request, drag rising and electrical device damages, which increases the costs.

Go as faster, economical and comfortable as possible always have been an imperative factor for passenger ferry transport and offshore operational support activities, for those reasons multiple options have been tested along the years in order to overcome the difficulties, already expressed, to sail across adverse sea states.

The foil assisted watercraft has been one of the better choices to improve the limited seakeeping of the fast catamarans, during the second half of the twenty century thousands of them were built, but due to some drawbacks, because the new of the technology, as remainder ship porpoising in big waves, limit speed for cavitation, additional hump drag at low velocities, ventilation by struts, complex efficient design and higher maintenance costs, then they did reduce their production, however, knowing the potential of hydrofoils to damp the longitudinal ship motion, improving the fast vessels seakeeping and performance and thanks to the recent advances and researches on this technology, they make that the

retrofitting existing catamarans with hydrofoils and building new hydrofoil-assisted multi-hulls are a booming industry today.[6]

The hydrofoil supported watercrafts are wing profiles under the water surface, installed on vessels with the aim to reduce the total hull drag through generate lift, as in an airplane, but in this case the area required by the foils is much lesser due to the water density is one thousand times higher than in the air. The lift generated as result of the foil water interaction makes the hull go up, either total or partially, reducing the displacement of the ship at cruise speed, which has several benefits such as: [1],[2],[3]

- ✓ Reduce the total hull resistance (up to 40%).[7]
- ✓ Motion damping effect at heave and pitch.
- ✓ Reduce the vertical acceleration (20% - 40%).[5]
- ✓ Improve the ride comfort in rough seas.
- ✓ Reduced wakes.
- ✓ Increased speed with existing engines (up to 40%).[7]
- ✓ Reduced fuel consumption
- ✓ Increased range for given storage.
- ✓ Reduced fuel storage for given range.
- ✓ Lower engine emissions.
- ✓ Lower propulsion power required.
- ✓ Reduced capital costs for propulsion system.

Thereby the hydrofoils become then in a good alternative to enhance the fast catamarans seaworthiness.

The main aim of this master thesis, is the exploration of the potential of foils to damp longitudinal oscillations and analyze if the retrofitting of existing catamarans improve their seakeeping and if it is worth economically.

In order to fulfill this propose two comparison analysis were made, calm water and seakeeping, both under two configurations, hull without foils and with them.

Based in Zarnick´s non linear formulation, the vertical acceleration estimations at sea state 1 and 2 were computed, both for a single hull case and the hull with hydrofoils support.

Making a comparison of the drag and power required in calm water, the heave and pitch RAO´s[1] and the vertical acceleration at CG obtained at the sea states analyzed, to show the benefits of hydrofoils was possible.

[1] RAO: Amplitude Response Operator

2. STATE OF THE ART

2.1 History & Developments

Since the Italian inventor *Enrico Forlanini* designed the first hydrofoil in 1906, showing its benefits in the performance and seaworthiness of the ships, the hydrofoils have been implemented in different watercraft either to civil or military applications.

The implementation of hydrofoils in fast catamarans started in 1974 with Soviet Union research done by *Yermotayev et al*. it was on planing catamaran hull forms with and without hydrofoil assistance comparison, then in the 80's, developments from USA and South Africa were made[1],[4].

Different prototypes were built, as the hydrofoil supported catamaran, HYCAT concept, JETFOIL by Boeing, SUPERJET series by Hitachi, 45.5m foil catamaran ferry by Hyundai, the F-CAT 40 by Daewoo and many others[4], some of them still working.

For instance the SUPERJET 30, *figure 1,* 80% is supported by the fully submerged foils, this catamaran with 32m LOA[2] and able to reach 35-40 knots, has demonstrated the advantages to be a hydrofoil assisted catamaran, specially for the favorable cost-performance, reliable safety and excellent seakeeping characteristics.[5] In order to improve the remainder porpoising in the fixed foil system, the SUPERJET has incorporated an automatic control system, ACS, which allows reduce the pitch motion and the vertical acceleration 20%[5] in comparison with conventional catamaran vessels, as is shown in *figure 2.*

[2] LOA: Length Overall

Figure 1- SUPERJET 30 Foil Catamaran[5]

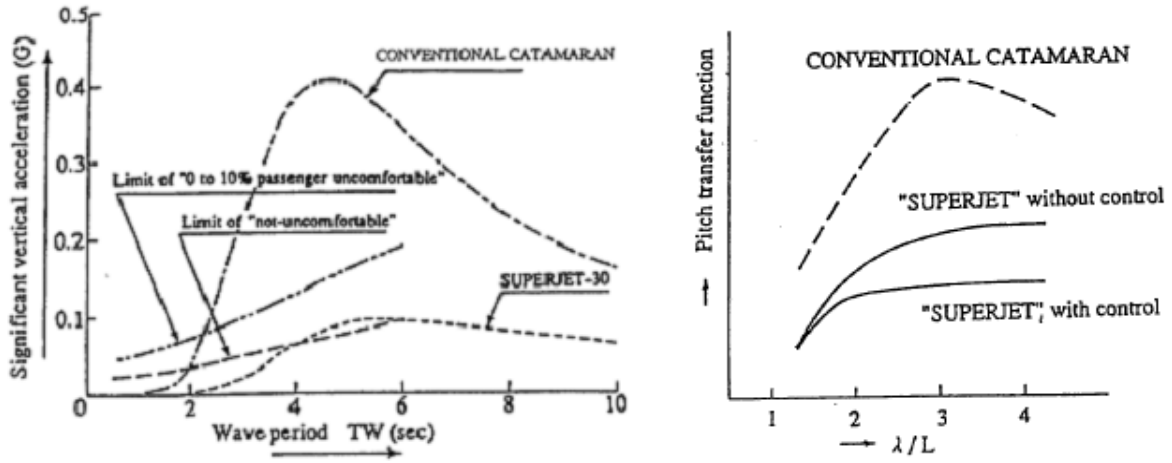

Figure 2 - Comparison of Vertical Acceleration and Pitch behavior between conventional catamaran and the SUPERJET foil assisted catamaran. [5]

In the *Hyundai* model the foils have controllable flaps, and have been placed in extreme fore and aft positions to maximize motion damping, the foils were intended to carry 40% of the displacement for both drag reduction and sea-keeping improvements, the original design needed additional foil refinement before it could be put into service.

The Daewoo model uses a single passive hydrofoil (NACA 66 section) just aft of the LCG below keel depth, the foil develops lift equal to 25% of the displacement and decreases the resistance by 15%, this allows an increase in speed of about 2.5 knots for the 42m vessel, bringing its maximum speed to 40 knots. Daewoo compared a number of hull designs and

found that a hard chine hull gave better resistance characteristics that the round bilge form, comparisons for the various hulls with and without foils show that the resistance is higher for the vessel with foils over a large portion of the speed range, the foil brings improvements from about 29 knots onward.[4]

The University of Stellenbosch through Dr. KGW. Hoppe developed the hydrofoil assisted ships and patented the HYSUCAT[3] for semi-displacement hull form catamarans and HYSUWAC[4] for larger semi-displacement type catamarans.[1]

The HYSUCAT consist in a hydrofoil member bridges the tunnel formed between two spaced demi-hulls of the craft in a position forward of the LCG of the craft. Two opposed hydrofoil trim tabs are positioned to the rear of the hydrofoil member and extend partially into the tunnel, one from each hull [2], as is appreciate in *figure 3.*

The HYSUWAC consist in a transverse hydrofoil member which bridges the demi-hulls of the catamaran, is disposed to the rear of the LCG, while opposed trim foils are provided to the front of the LCG, extending partially into the tunnel from each demi-hull, this setting is shown in *figure 3.*

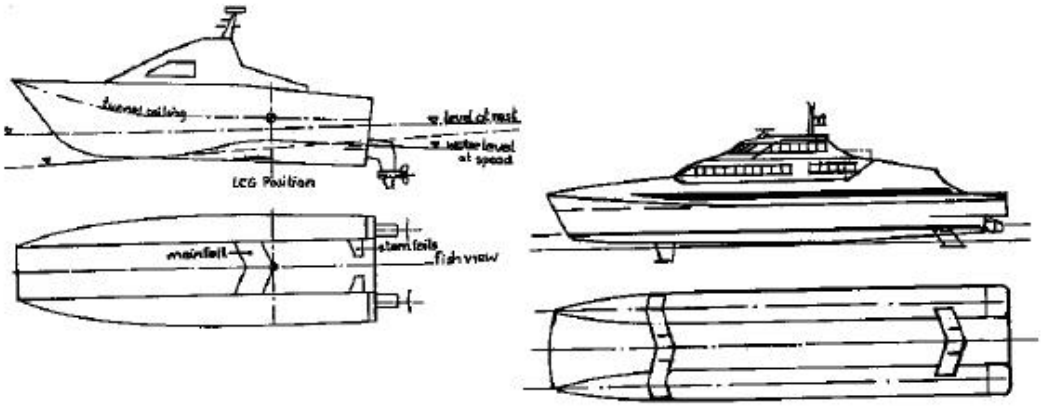

Figure 3 - HYSUCAT Configuration (Left) / HYSUWAS Configuration (Right)

[3] HYSUCAT: Hydrofoil Supported Catamaran
[4] HYSUWAC: Hydrofoil Supported Watercraft

More than 200 HYSUCAT have been built, this technology has allowed to enhance the total hull resistance and the maximum speed up to 40%.[4] The HYSUCAT and HYSUWAC concepts have not been used only as new design, the retrofitting of conventional catamaran has been successfully implemented also, how is the case of the UK *Prout Panther 64* catamaran in 1998, which after the foils were installed, it shown increases of 40% in its top speed. [7]

Figure 4 - Prout Panther 64 Retrofits Foil Assisted Catamaran

2.2 Hydrodynamics and Resistance Principles

The hydrodynamics and resistance principles of hydrofoils assisted catamarans are strongly influenced by the correctly foil and hull design, the foils allow that the hull rise out the water, unload it and decreasing the hull resistance at cruise speed, because the reduction of the wetted area and the hull wave making, is important take into account the added resistance due to the foils and hull/foils interaction also. The *figure 5* describes a breakdown resistance for a hydrofoil assisted catamaran, where is possible to observe the frictional and residual components produced by the hull, the foil and how they interact each other. [1],[4]

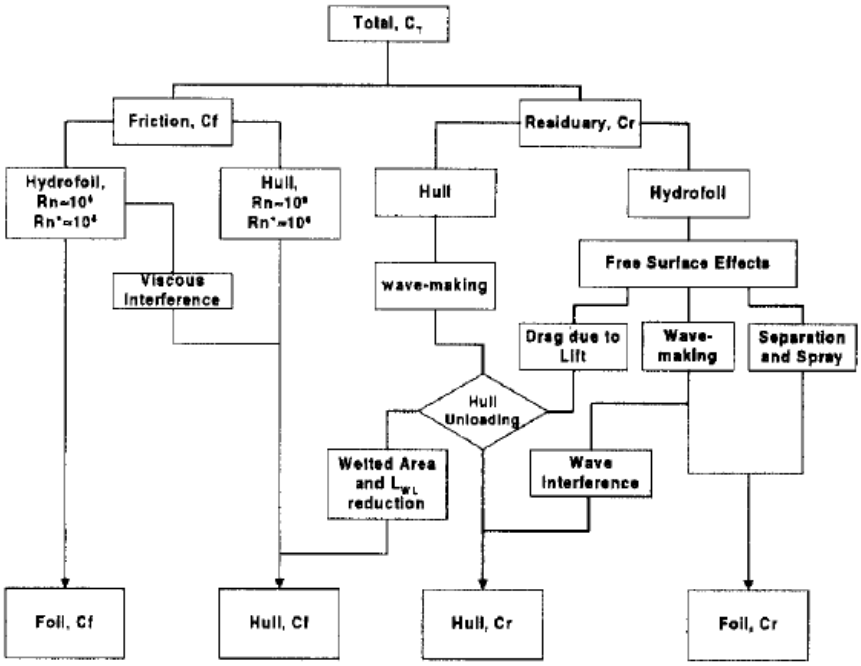

Figure 5 - Breakdown Resistance for Assisted Foil Catamaran

The *figure 6* exposes the hump drag at take off stage and the higher performance at cruise speed that the hydrofoil craft are able to reach in calm water. The hydrofoil add resistance to the hull, mostly during the take off phase, however the net reduction in overall resistance due to the reduced wetted area is significant, and can be up to 35% in calm water compared to the resistance of the hull without a hydrofoil[9], therefore to assist a catamaran by foils, the operational velocity range is an important parameter to define its suitability.

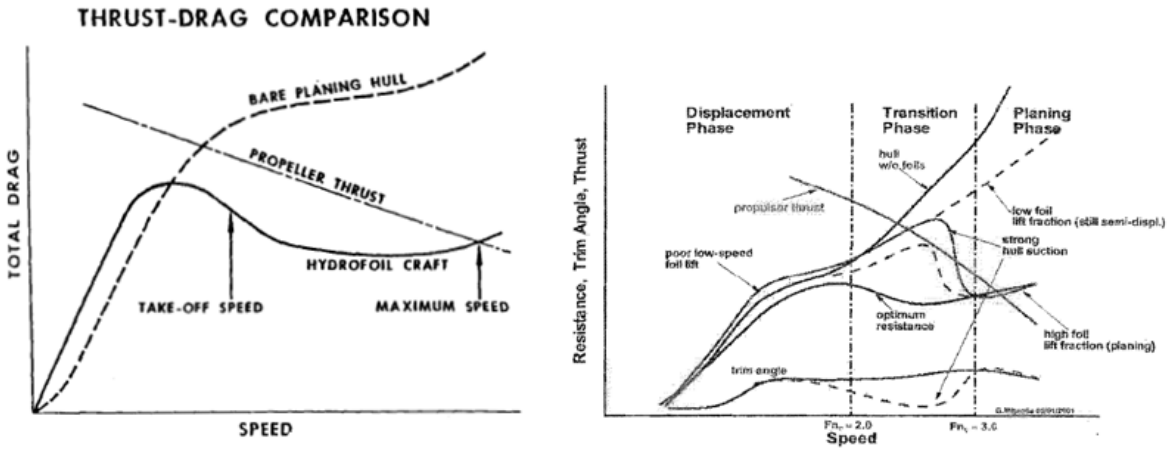

Figure 6 - Typical Calm-Water Thrust-Drag Curves

Normally the hydrofoil assistance does not make sense for vessels operating below the displacement hump, volumetric froud number, Fn around 1.5. Since the weight of a craft is proportional to the cube of a linear dimension and the lift to the square of the linear dimension, the required size for a foil system out grows practical sizes for these speeds, therefore Fn=1.5 is the most general limit where the hydrofoil assistance is useful to improve the hull resistance. [1]

Although the major efficiency that the foils provide is at cruise speed, there are some options to improve their efficiency at lower velocities, as the HYSUWAC configuration, doing lift off the bow before to take off, because the foil in front, decreasing the wetted area quickly, to keep the struts as much as possible outside the water or install retracted foils, at low speed the hydrofoils would be stowed, to avoid the added foil resistance and when the vessel overcome the hump drag the hydrofoils would be deployed in order to take chance of their benefits on longitudinal ship motion damping, better performance and comfortable rides.

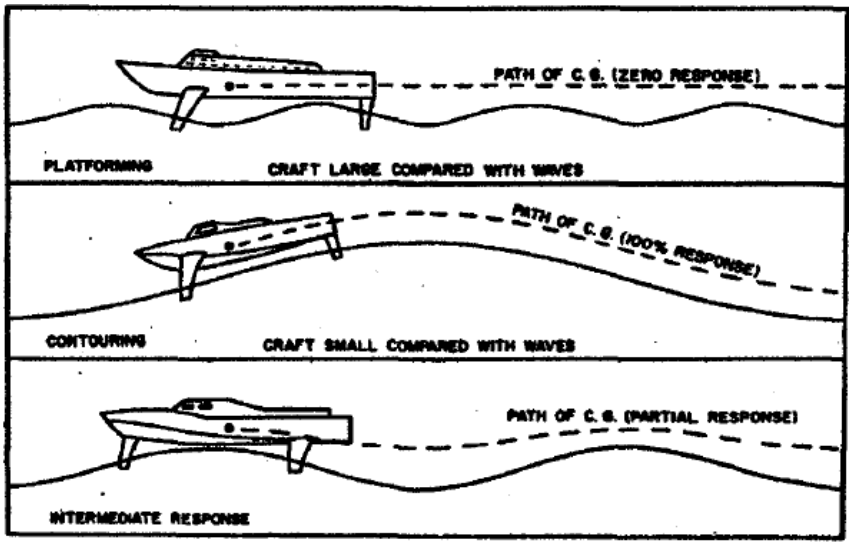

Figure 7 - Typical Hydrofoil Flight Modes

At cruise speed, there are mainly, two modes in which the ship can operate in rough water as shown in *figure 7*. If the hydrofoil is relatively large compare with the waves and its flying height is sufficient to permit the hull to travel in straight and level flight clear of the waves, the craft is said to "platform" with zero response. In the other extreme, if the hydrofoil is small compare to the waves, it is constrained to follow the surface. This is known as

"contouring". and ideally, a 100% response is required. With a hydrofoil having an autopilot and the ability to control lift, one has the option to select reasonable compromises between these two extremes and seek to provide minimum foil broach and maximum hull clearance without exceeding specified limits of craft motion and accelerations.[10]

2.3 Hydrofoil Improve the Seaworthiness

The hydrofoils are very effective for damping ship´s motion, the heave and pitch transfer function, in head seas, are very small, depending of the sea state level the wave orbital motion and the ship´s motion itself change the foil angle of attack, this change is greater in following seas than in head ones, this difference arise from the fact that the phase of orbital motion and ship´s motion are almost equal in following waves[5].

As was described above, the fixed hydrofoil enhance the ship seakeeping by damping effect, even they can increase the ship performance. The incorporation of an automatic control system, as in the SUPERJET it is a good option in order to optimize the damping effect of the hydrofoils in a higher range of sea states.

In the 90´s, a Norwegian FOILCAT[5] experiment showed, by simulation regarding to effectiveness of its control system, to reach vertical acceleration of 0.062g at 43 knots in sea state 5, which is a good agreement in sea trials[10] as is illustrated in *figure 8,* where is described the human response at vertical acceleration exposures.[11]

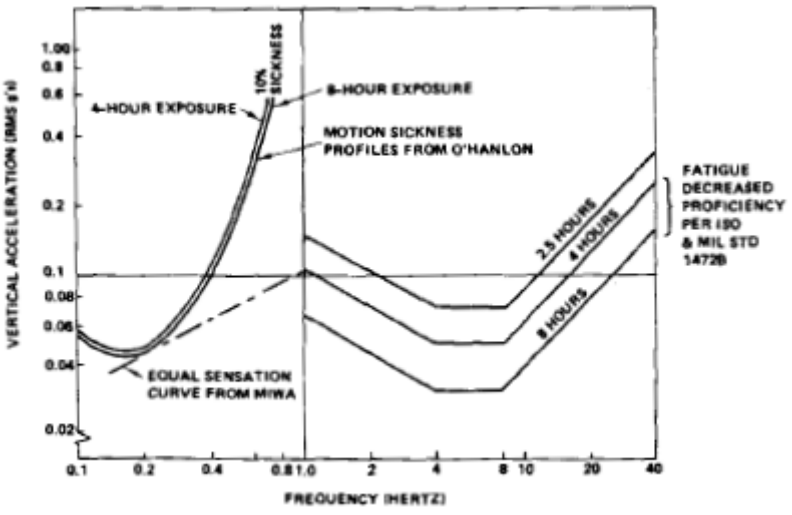

Figure 8 - Data Base for Human Response to Vertical Acceleration

[5] FOILCAT: Foil Catamaran

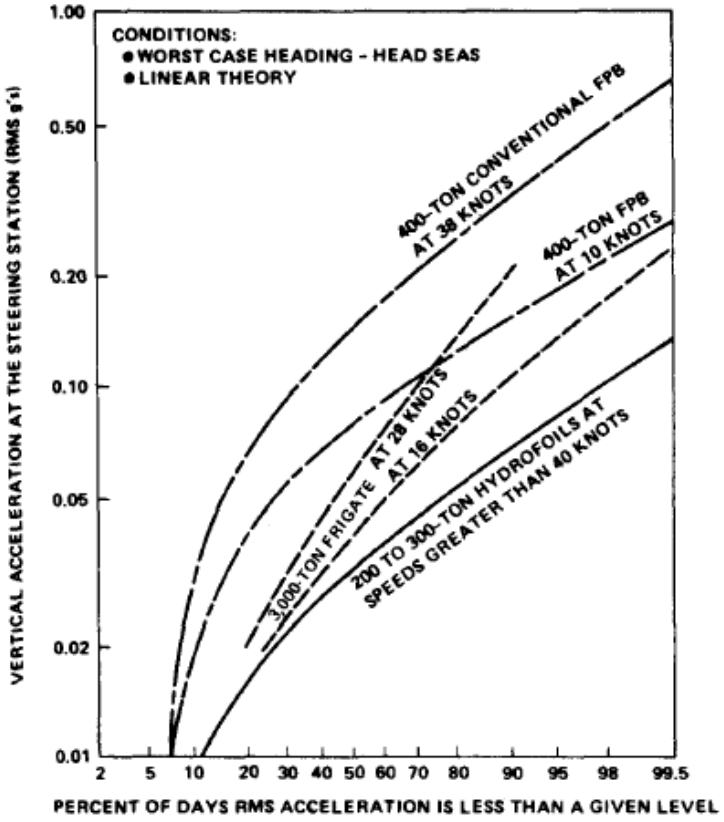

Figure 9 - Long-Term Vertical Acceleration Distributions in the North sea

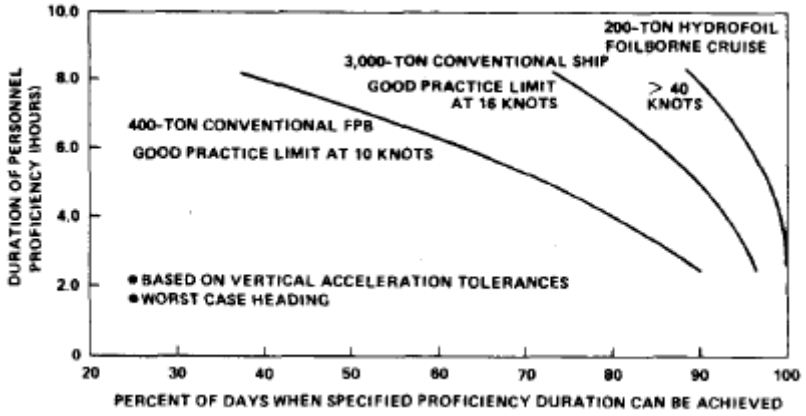

Figure 10- North Sea Working Environment (All Seasons)

The *figures 9 and 10* expose a comparison of hydrofoils with conventional ships about the quantity of days that they can produce less vertical accelerations under North sea conditions and how long they can keep their crews under vertical acceleration tolerance levels, as the

hydrofoils are able to have lesser vertical acceleration during more time, therefore their crews and passengers can be longer time sailing within comfort ride conditions. [11]

The automatic control system is the most used to improve the performance of the foils in rough seas, it is considered as an active system, however there are another systems that could be vanish the still foil porpoising, such springs devices attached to the fixed foils in order to maximize their damping effect in the ship motion[12], and a mechanical angle of attack changed device through a buoy located in the front foil, which is coupling with a hinge, with the aim to vary its angle of attack while it follow the incoming head waves producing more lift when the waves have more amplitude, these alternatives are called passive systems.

2.4 Hydrofoil Design

To design a hydrofoil is important to know that each project need its own research, because there are not fixed rules to determine a general behavior.[4]

The appropriate hydrofoil design has a big influence in the improvement of the seakeeping ship behavior, depending of the mission profile of each FOILCAT, then it will be its hydrofoil design, specially for retrofits FOILCATs, because in this case the foil system has to be designed to match with an existing hull, and this often results in a foil configuration that is less than the optimal one, nevertheless it can brings substantial improvements in resistance.[4]

One of the most significant parameters to hydrofoil design are the foil loading, the foil position and the foil configuration.

The foil loading could be from 25% in single wing up to 100% in multi wing settings, the better resistance improvements are given by arrangements that support as much of the load on the foils, the foil load depends of the propulsion, cavitation limits, position of LCG and stability considerations.[4]

While the major foil loading provides better hull resistance performance, also it means that the entire ship stability will be determined mostly by the foils instead by the hydrodynamics hull ship features, because it will be totally outside the water, In this case an automatic control system installed on the foils is recommended.

Besides is important to consider, especially in retrofits foil catamaran, the foil loading percentage, because as more the foil is load, the propulsion can go to be ventilated, so one have to find the higher efficient point between enough foil loading to decrease as much as possible the hull resistance and avoid the propulsion ventilation. [13]

Cavitation can usually be avoided with the aid of the correct foil profiles, sweep, and span wise variation of camber and angle of attack. The limit speed due to cavitation problems, now can be overcome using supercavitation profiles, which could to reach higher velocities, 60 knots and even more. [4]

The foil position depends if is a retrofits catamaran or a new design, model tests at the University of Stellenbosch have shown that incorrect foil positions in relation to the LCG can result in the vessel becoming unstable in pitch and yaw or simply do not bring the desired resistance improvements. The best foil positions for resistance improvements are often close to the stability limits of the vessel.[4]

Previous investigation[1] and the foil assisted catamaran by Hyundai, suggest that a longer distance between rear and front foils could be the optimal one in order to avoid the downwash disturbing water flow over the rear foils members, another solution could be to locate the front and rear foil no aligned, respect to the horizontal keel level, this setting would have influence in the porpoising behavior also.

The foil configuration more common are shown in *figure 11*. The tandem configuration seems to be the most popular, this is most likely for simplicity, and the fact that it allows a large proportion of the vessel load (up to 100%) to be carried efficiently on the high aspect ratio foils, also because is less sensitive to LCG shifts and overloading.

The airplane configuration or its simpler version, the mono-foil, have found much application in planing vessels with resistance improvements of up to 40% being achieved on HYSUCATS, but is limited for the lift capability at semi-displacement speed.

The canard configuration, used successful in large semi-displacement ships, allows a large percentage (up to 100%) of the vessel weight to be carried on the foils, bow foil vertical struts can also double as steerable surfaces if necessary, tests done at the University of Stellenbosch have indicated that the canard system brings resistance improvements from Froude numbers as low as 1.0 in some cases without any increase in resistance for speeds below that.[1][4]

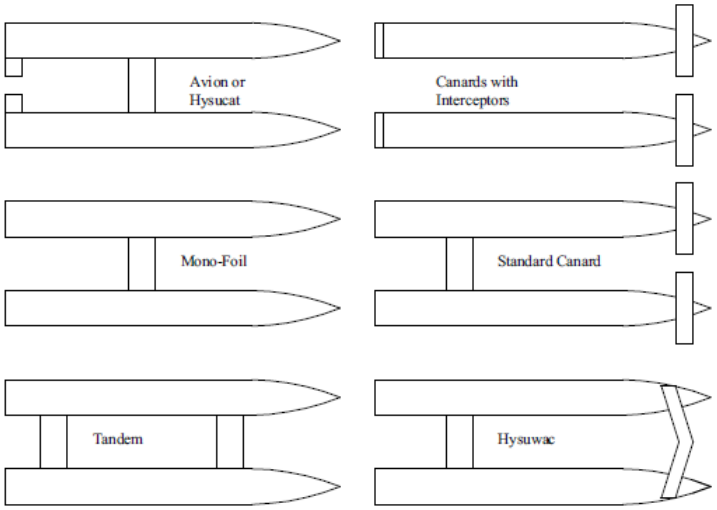

Figure 11 - Typical foil configuration

The influence of foil angle of attack is small on its damping effectiveness, Zero angle of attack seems to be the best.[3]

The calculation of the lift and drag by the foils is widely known and in order to be more precise in the estimations, some authors propose reduce the lift generated taking into account the water free surface and the changes in the angle of attack due to wave orbital motion and ship's motion[5].

The suitable hull design will determine the corrected perception of the hydrofoil advantage, because a non correct hull form can delete the foil effect due to the hull foil interaction and the hull behavior itself.

Is important to design a new hydrofoil assisted catamaran or retrofit someone existing focused to improve the seakeeping reaction qualities on waves excitations, such as vertical accelerations at bow and at LCG, heave and pitch damping and lesser added resistance in waves.[3]

Determination of hydrodynamic coefficients by experimental approach is costly, and requires meticulous laboratory equipment; therefore, utilizing numerical methods and developing a virtual laboratory seems highly efficient, one of the most recent studies to determine the coefficients of longitudinal motions of a planing catamaran with and without a hydrofoil was done using RANS method to evaluate the foil effects on them, where was demonstrated numerically the damping benefits of the foil to improve the catamaran seakeeping and performance. [14]

3. BASELINE MATHEMATICAL MODELS

To compute the calm water conditions and the seakeeping behavior of the ship, the following mathematical models were used.

3.1 Savitsky´s Planing Hull Empirical Formulation

In order to do the calm water analysis of a planing hull with and without foils assistance and determine the initial trim and sinkage position, necessary for the initial conditions of the seakeeping analysis, the Savitsky´s planing hull empirical formulation was applied, this model is well described in reference [15] and the equations implemented are in detail in section 5.1.2

3.2 Zarnick´s Estimation of Vertical Acceleration Method

To estimate the vertical accelerations of the catamaran in waves, with and without foils, the Zarnick´s non linear mathematical model was employed, this formulation is well defined in reference [16] and the equations implemented are in detail in section 6.1.2. The Zarnick´s formulation is based in the added mass and strip theory.

3.3 Lift Force in a Submergence Foil

To incorporate the influence of the foils, the Zarnick´s model was extended taking into account the equation 1.[5]

$$F_{foil} = \frac{1}{2}\rho U^2 S C_{l\alpha}(\theta_e - \theta_0) + m_{af}(\dot{w}_z + x_f\ddot{\theta} + \ddot{Z}) \qquad (1)$$

Where the foil added mass is:

$$m_{af} = \frac{\pi}{2} + \frac{FoilChord^2}{4} \times FoilSpan \times \rho \qquad (2)$$

And the effective angle of the foil due to ship´s and wave orbital motion is:

$$\theta_e = \theta + \frac{w_z - x_f\,\dot{\theta} - \dot{Z}}{U} \qquad (3)$$

4. CATAMARAN DESCRIPTION

4.1 Hull Features

The table 1 summarizes the main geometrical hull characteristics.

Table 1. Hull Features

Item	Value	Units
Mass	60.000	kg
Length	20	m
Beam	4	m
Draft	0.72	m
Distance among Hulls	4	m
Length/Beam	5	----
Deadrise	20	°
LCG	1/3 of Length	m
VCG	30% of Beam	m
Radius of Gyration	25% of Length	m
Horizontal Velocity	26.83	m/s

4.2 Foil Features

The tandem foil configuration was used, both foils were located at the same distance from CG, equivalent at LCG magnitude value and at same level of the keel. The foil shape is as rectangular wing, where the span is equivalent to the distance between hulls.

The foil surface was defined according with the foil load defined, 80% of the hull displacement, the depth of submergence and the thin foil theory, the equation 4 allows estimate that value.

$$S = \frac{2 \times W \times FoilLoad\%}{\rho U^2 C_l} \qquad (4)$$

Where Lift Coefficient is function of foil submergence, h [1]

$$C_l = C_{l\alpha}\,\theta\left(1 - \frac{\left(\sqrt{4h^2+1} - 2h\right)^2}{2}\right) \qquad (5)$$

As the distance among hulls is 4 m and submergence is the equilibrium hull draft, thus the foil chord is 0.25 m.

Table 2 - Foil Features.

Foil load [%W]	Span [m]	Chord [m]	Submergence h [m]	Distance to CG x_f [m]
40 each one	4	0.25	0.72	LCG both sides

5. CALM WATER ANALYSIS

5.1 Hull Without Hydrofoils Support

5.1.1 Assumptions Done

The main assumption done in this chapter was that all forces pass through CG, as is described in figure 12.

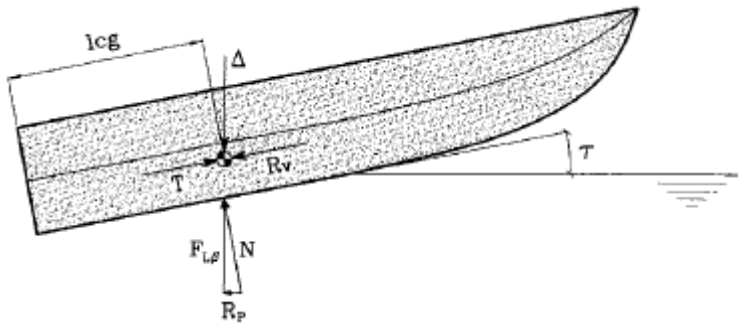

Figure 12- Forces Through CG

5.1.2 Mathematical Formulation Used

Since all forces pass through CG, the next set of equations determine the trim, sinkage, hull drag and power required of the catamaran study object. To solve some of them, the *Newton-Raphson* numerical method was implemented.

$$\frac{LCG}{\lambda_w B} - 0.75 + \frac{1}{5.21\frac{Fn_B^2}{\lambda_w^2} + 2.39} = 0 \qquad (6)$$

$$C_{l\beta} = \frac{W}{0.5\rho U^2 B^2} \qquad (7)$$

$$C_{l\beta} = C_{l0} - 0.0065\beta C_{l0}^{0.6} \quad (8)$$

$$C_{l0} = \tau rim_{deg}^{1.1}\left(0.012\lambda_w^{0.5} + 0.0055\frac{\lambda_w^2}{Fn_B^2}\right) \quad (9)$$

$$\frac{B}{2} = \frac{\pi}{2tan\beta}x_s\tau rim \quad (10)$$

$$l_c = \lambda_w B - 0.5x_s \quad (11)$$

$$l_k = 2\lambda_w B - l_c \quad (12)$$

$$Draft_{transom} = l_k \sin(\tau rim) \quad (13)$$

For the resistance and power requeried:

$$Resistance = R_{frictional} + R_{induced} \quad (14)$$

Where:

$$R_{induced} = W\tau rim \quad (15)$$

$$R_{frictional} = 0.5\rho C_f S_w U^2 \quad (16)$$

With,

$$C_f = \frac{0.075}{(\log_{10} Re - 2)^2} + 44\left[\sqrt[3]{\frac{150\times10^{-6}}{l}} - \frac{10}{\sqrt[3]{Re}}\right] + 0.125 \quad (17)$$

$$S_w = \frac{tan^2\beta}{sin\beta}\left(\frac{B^2}{8\tau rim}\right) + \frac{B}{cos\beta}l_c \quad (18)$$

Thus power is equal to,

$$Pow = Resistance \times U \quad (19)$$

5.1.3 Results

The table 3 contains the planing hull features without foils.

Table 3- Calm Water results NO foils.

Item	Value	Units
Trim	5.5	°
Draft at transom	1.5	m
Resistance	91.2	KN
Power	3282	hp

5.2 Hull With Hydrofoil Support

5.2.1 Assumptions Done

To determine the initial equilibrium position, the resistance generated and power required with hydrofoils configuration the following assumptions were contemplated.

- ✓ The mass of the foils are neglected to be small compared with the ship mass.
- ✓ The symmetry of the foils makes null the net momentum generated each others.
- ✓ Both foil submergences are equal and at the same level of the hull keel.
- ✓ The chine beam stills submerge.
- ✓ To simulate the action of the foils on the hull, the Savitsky´s methodology described in section 5.1.2 was applied under the same parameters as without foils, with the note that displacement, to compute the lift hull coefficient C_{LB} , is now the initial one times the foil load defined.

5.2.2 Mathematical Formulation Used

The mathematical model is the same as section 5.1.2, with the difference that now the equation 7 is replaced by equation 20.

$$C_{l\beta} = \frac{W \times FoilLoad\%}{0.5\rho U^2 B^2} \qquad (20)$$

5.2.3 Results

The table 4 holds the planing hull features with foils.

Table 4 - Calm Water results with foils.

Item	Value	Units
Trim	1.7	°
Draft at transom	0.77	m
Hull Resistance	51.66	KN
Foil Resistance	1.84	KN
Total Resistance	53.5	KN
Power	1926	hp

5.3 Comparisons

As the hull is raised to an higher position from the still water line, due to foil action, the hull wetted surface resultant is lesser, therefore the hull drag is reduced 43.35%.
For the total drag, one has to add the foil resistance generated, which is really small one and the total drag still be minor than the total drag without foils. With foils, the total drag and the power are reduced more than 40%.

In table 5 and graphics 1,2 is possible to observe the resistance and power improvements achieved by foils support.

Table 5 - Resistance and Power reduction due to the foils assistance

Item	Value	Units
Total Drag No Foils	91.2	KN
Total Drag With Foils	53.5	KN
Power No Foils	3282	hp
Power No Foils	1926	hp
Reduction	41.33	%

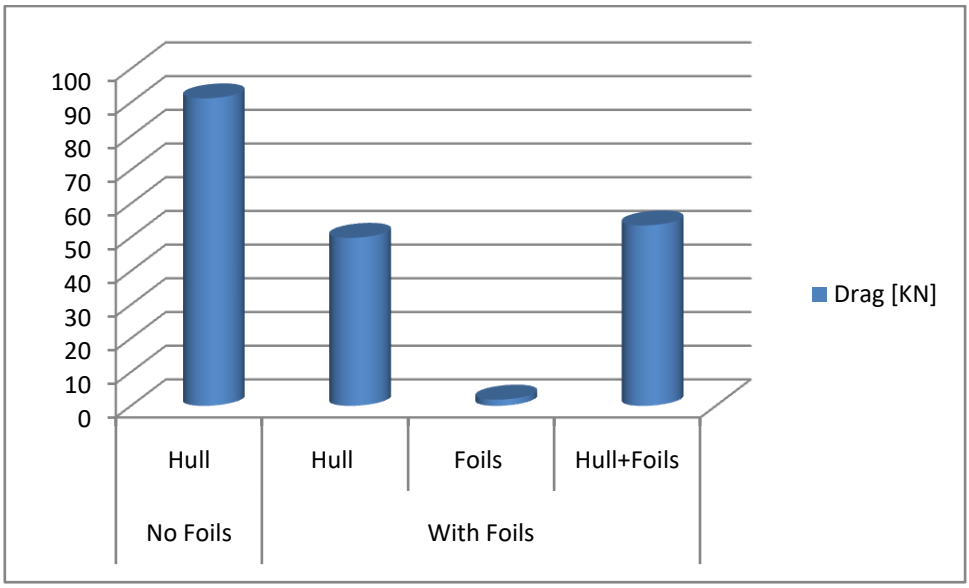

Graphic 1 - Resistance Comparison

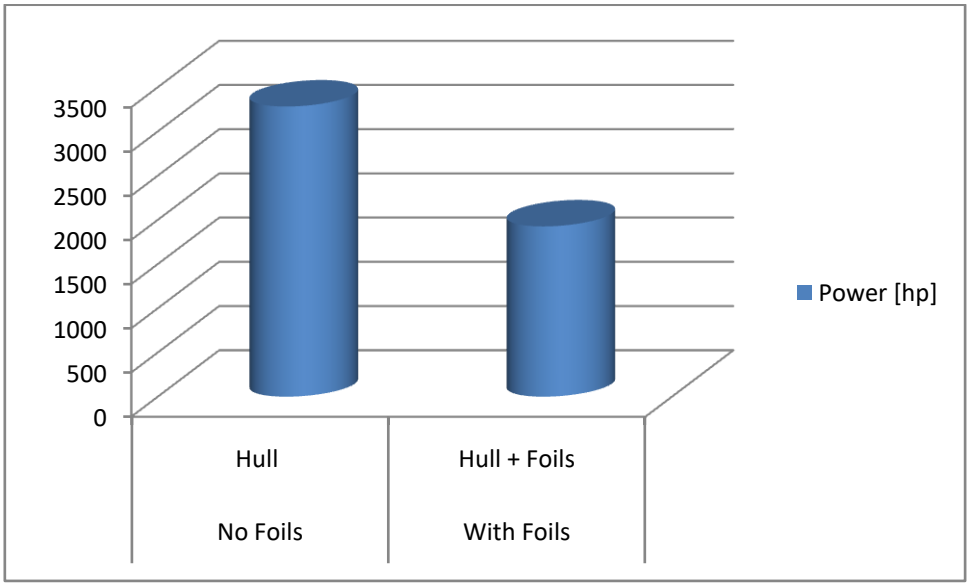

Graphic 2 - Power Comparison

6. SEAKEEPING ANALYSIS

6.1 Hull Without Hydrofoils Support

6.1.1 Assumptions Done

In order to apply the Zarnick´s formulation to estimate the vertical acceleration and heave and pitch longitudinal oscillation, the following assumptions were defined.

- ✓ Potential flow scope, therefore added mass and airy waves theories take place.
- ✓ All forces pass through CG.
- ✓ The horizontal velocity is constant on time.
- ✓ The initial heave and pitch positions come from the previous calm water analysis.
- ✓ The longitudinal oscillation are caused by alteration of the wetted geometry due to the geometrical proprieties of the wave and the vertical orbital velocity component, the influence of its horizontal component are neglected to be small in comparison to the hull horizontal velocity.
- ✓ The wavelengths have to be greater or equal than the hull length.
- ✓ The wave slope has to be small, E<0.25
- ✓ The hull length/beam relationship has to be higher or equal than 3.
- ✓ The range of velocity/square root hull length relationship has to be among 4 and 6.
- ✓ The spray effect at hull bow is no taken into account.
- ✓ The thrust and drag are neglected to be small in comparison with the hydrodynamic forces.
- ✓ The orbital velocity is taken at non disturbed free surface Z=0.

The figure 13 describes the seakeeping movement analyzed.

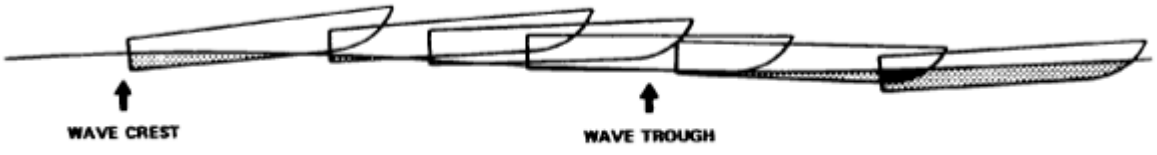

Figure 13 - Hull trajectory in waves

6.1.2 Mathematical Formulation Used

The frames of reference used are described in figure 14. One fix to earth and other one at CG of the ship.

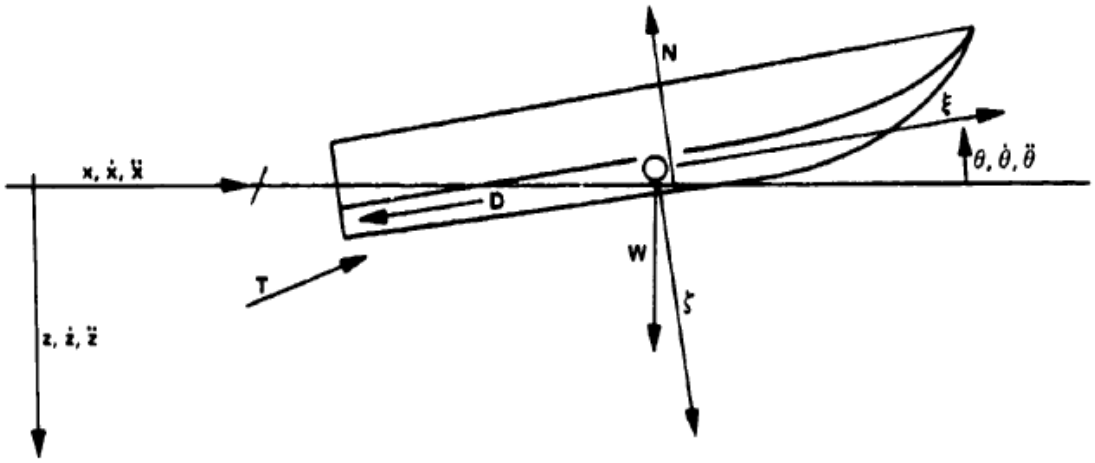

Figure 14 - Frames of Reference

At any point P(ξ,ζ) the values of X and Z are determined by:

$$X = X_{cg} + \xi\cos\theta + \zeta\sin\theta \qquad (21)$$

$$Z = Z_{cg} - \xi\sin\theta + \zeta\cos\theta \qquad (22)$$

Taking into account the previous assumptions the equation of motions remains as:

$$(M + M_a cos^2\theta)\ddot{Z}_{cg} - (Q_a cos\theta)\ddot{\theta} = F_z^* + W \qquad (23)$$

$$-(Q_a cos\theta)\ddot{Z}_{cg} + (I + I_a)\ddot{\theta} = F_\theta^* \qquad (24)$$

Where the added mass, momentum and added mass pitch inertia are,

$$m_a = k_a \frac{\pi}{2}\rho b^2 \qquad (25)$$

$$M_a = \int_0^l m_a d\xi \qquad (26)$$

$$Q_a = \int_0^l m_a \xi d\xi \qquad (27)$$

$$I_a = \int_0^l m_a \xi^2 d\xi \qquad (28)$$

The hydrodynamic forces are defined by,

$$\begin{aligned} F_z^* = cos\theta \Big\{ & M_a \dot{\theta}\left(\dot{Z}_{cg} sin\theta - \dot{X}_{cg} cos\theta\right) \\ & + \int_0^l m_a \frac{dw_z}{dt} cos\theta d\xi \\ & - \int_0^l m_a w_z \dot{\theta} sin\theta d\xi - \int_0^l m_a V \frac{\partial w_z}{\partial \xi} sin\theta \, d\xi \\ & + \int_0^l m_a U \frac{\partial w_z}{\partial \xi} cos\theta \, d\xi - UV m_a|_{stern} - \int_0^l V \dot{m}_a \, d\xi \\ & - \int_0^l \rho C_D b V^2 \, d\xi \Big\} + \int_0^l a_{BF} \rho g A d\xi \end{aligned} \qquad (29)$$

$$\begin{aligned} F_\theta^* = & -Q_a \dot{\theta}\left(\dot{Z}_{cg} sin\theta - \dot{X}_{cg} cos\theta\right) \\ & - \int_0^l m_a \frac{dw_z}{dt} cos\theta \xi d\xi \\ & + \int_0^l m_a w_z \dot{\theta} sin\theta \xi d\xi + \int_0^l m_a V \frac{\partial w_z}{\partial \xi} sin\theta \, \xi d\xi \\ & - \int_0^l m_a U \frac{\partial w_z}{\partial \xi} cos\theta \xi \, d\xi + UV m_a \xi|_{stern} + \int_0^l UV m_a d\xi \\ & + \int_0^l V \dot{m}_a \xi \, d\xi + \int_0^l \rho C_D b V^2 \xi \, d\xi \\ & + \int_0^l a_{BM} \rho g A cos\theta \xi d\xi \end{aligned} \qquad (30)$$

Where the horizontal and vertical velocities are,

$$U = \dot{X}_{cg} cos\theta - \left(\dot{Z}_{cg} - w_z\right) sin\theta \qquad (31)$$

$$V = \dot{X}_{cg} sin\theta - \dot{\theta}\xi + \left(\dot{Z}_{cg} - w_z\right) cos\theta \qquad (32)$$

The orbital velocity is defined as,

$$w_z = \eta_0 \omega e^{kz} \sin(kx - \omega t) \qquad (33)$$

The change in the added mass and the vertical acceleration perpendicular to the baseline are,

$$\dot{m}_a \approx k_a \pi \rho b (0.5\pi cot\beta) \frac{\left(\dot{Z}_{cg} - \dot{\eta}\right)}{cos\theta - \dot{\eta} sin\theta} \qquad (34)$$

$$\dot{V} = \ddot{Z}_{cg} cos\theta - \ddot{\theta}\xi - \dot{w}_z cos\theta + \dot{\theta}\left(\dot{X}_{cg} cos\theta - \dot{Z}_{cg} sin\theta\right) + w_z \dot{\theta} sin\theta \qquad (35)$$

Where the wave elevation is,

$$\eta = \eta_0 \cos(kx - \omega t) \qquad (36)$$

Thus, the second order couple differential equations are expressed in the following matrix arrangement,

$$\begin{bmatrix} M + M_a cos^2\theta & -(Q_a cos\theta) \\ -(Q_a cos\theta) & (I + I_a) \end{bmatrix} \begin{bmatrix} \ddot{Z}_{cg} \\ \ddot{\theta} \end{bmatrix} = \begin{bmatrix} F_z^* + W \\ F_\theta^* \end{bmatrix} \qquad (37)$$

The matrix system can be solved as the linear system, $X = A^{-1}B$

The Runge Kutta 4°order to second order couple differential equation was employed to solve the matrix system, where the initial condition were defined by the Savitsky´s method previously, the trapezoidal numerical method to solve the integrals was used. The convergence of the method was achieved at delta time of 0.01.

A C++ code was programmed to solve the matrix system, it can be observed in the appendices.

The hull was divided in 21 sections, the integrals were evaluated along the length ship, where its computation was conditioned by the depth of submergence of each segment, this due to each strip taken has a different dynamic conditions at every time step.

At determined time the hull bow is outside the water, considered dry, therefore no forces are exerted there, downwash, from the point of match among the free surface and the hull until the chine, is considered as dry chine section, where the added mass changes on time and length hull, because the slamming and the wetted beam changes, continuing downwash in the hull up to the transom, is considered as wetted chine, here the added mass takes its maximum value and is constant.

The submergence of each section is defined as, $h = Z - \eta$

The figure 15 illustrates the hull section division.

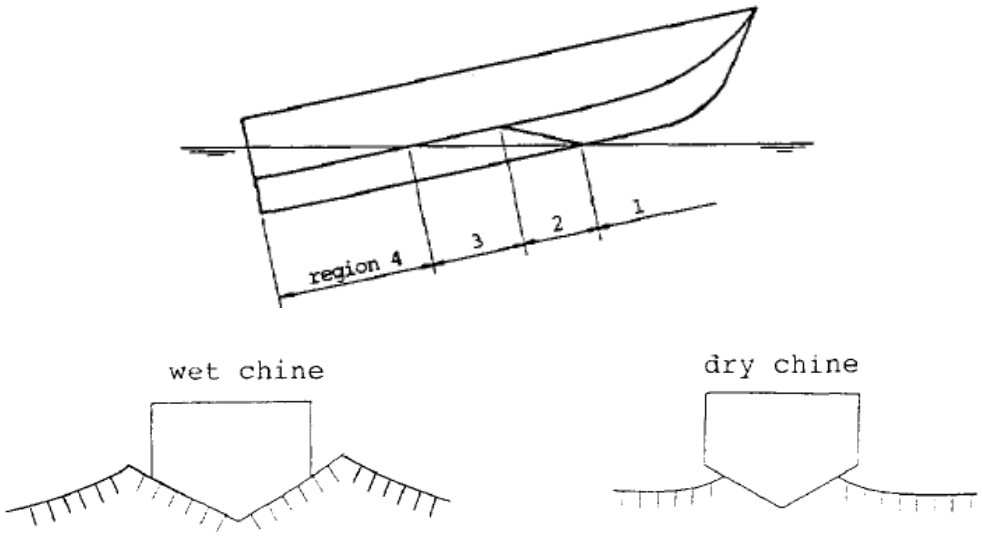

Figure 15-Flow regions and conditions along the hull [17]

6.1.3 Sea State 1 Results

The simulations were done at 52.15 knots, Beam Froude Number of 4.28, that it is mean fully planing condition and with different wavelength/hull length relationships such as 1,1.5,2,3,4 and 5. The wave amplitude used to represent the sea state 1 was 0.3 meters.

A sample of the heave, pitch and vertical acceleration behavior on time is presented in graphics 3,4,5.

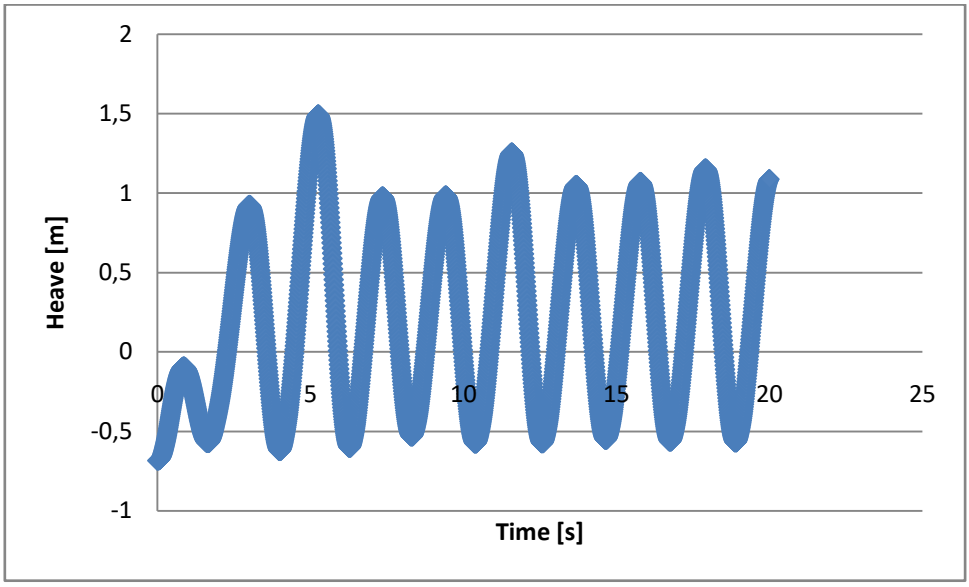

Graphic 3- Heave Behavior in time at 26.83 m/s, wave amplitude of 0.3 m and wavelength twice the hull length.

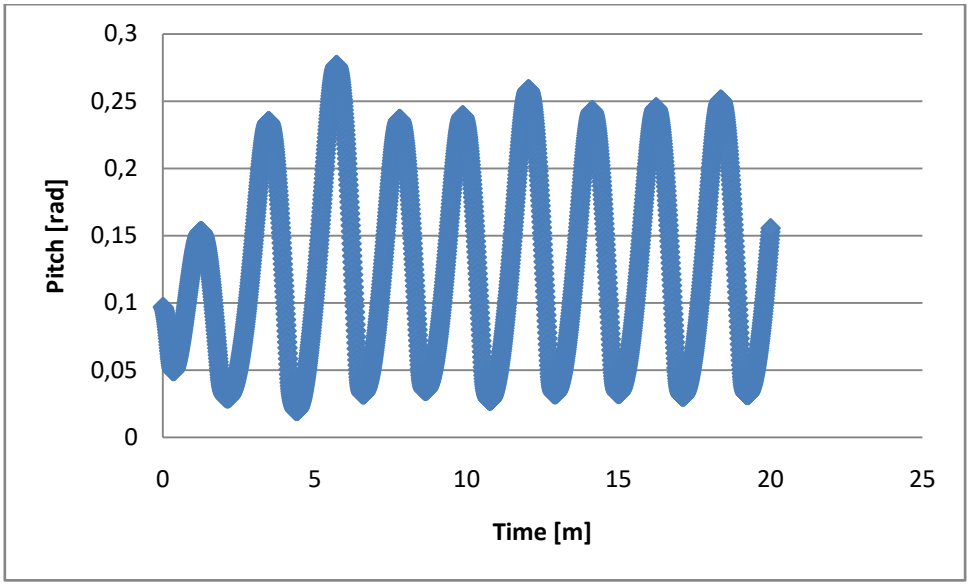

Graphic 4 - Pitch Behavior in time at 26.83 m/s, wave amplitude of 0.3 m and wavelength twice the hull length.

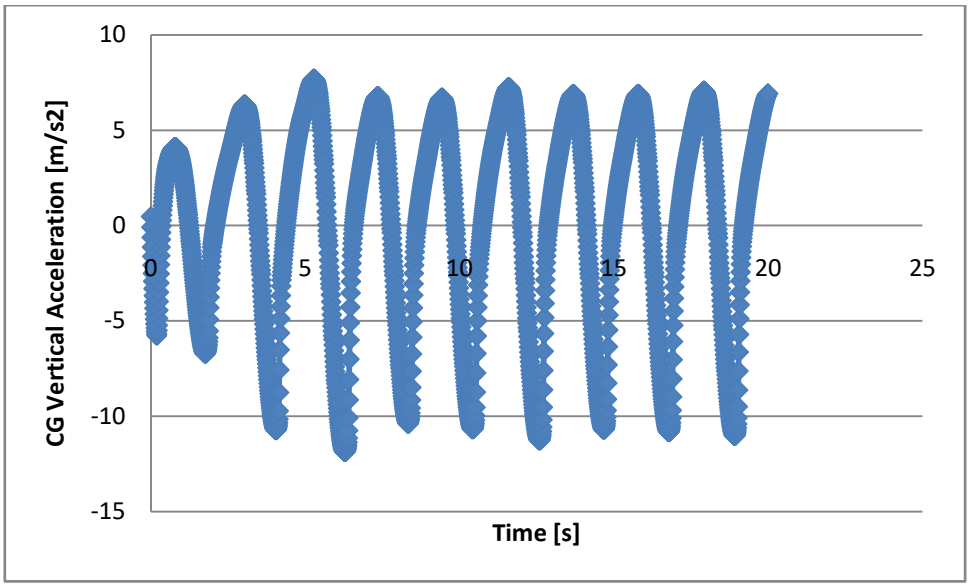

Graphic 5 - CG Vertical Acceleration behavior in time at 26.83 m/s, wave amplitude of 0.3 m and wavelength twice the hull length.

The longitudinal pitch and heave oscillation and the vertical acceleration at CG are shown in graphics 6,7,8. The mean run time was 20 seconds, in order to avoid noise data only the last two seconds were used. The double heave and pitch amplitudes were obtained by averaging the crest and trough values and making the difference between them, for vertical acceleration the more negative value was taken.

The doubles amplitudes were normalized by the double amplitude of the wave, for heave motion, by twice the wave slope for the pitch and by the gravity in the vertical acceleration case.

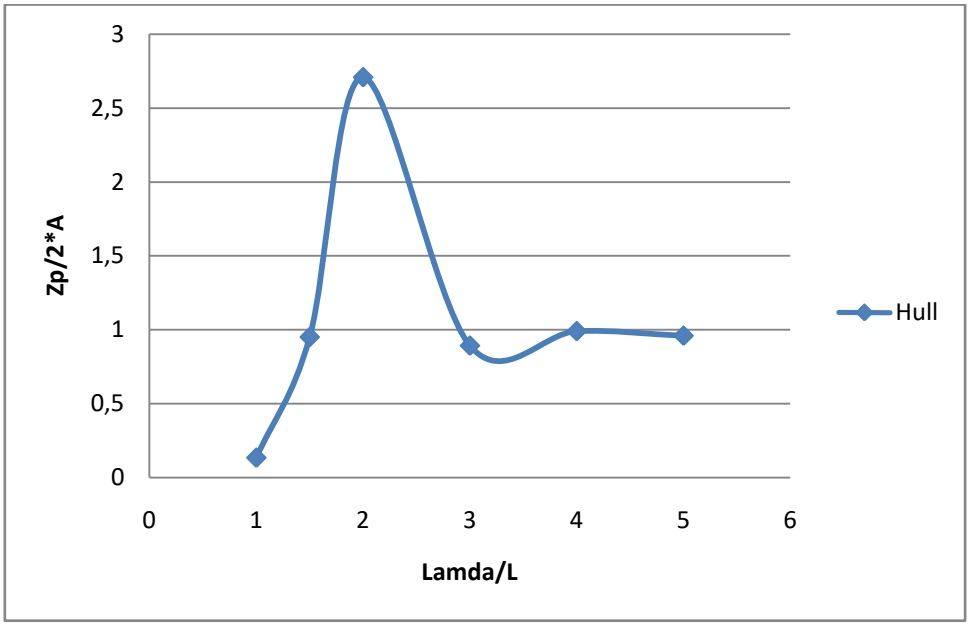

Graphic 6 - Heave RAO at 26.83 m/s, wave amplitude of 0.3 m and different wavelength/hull length relationships.

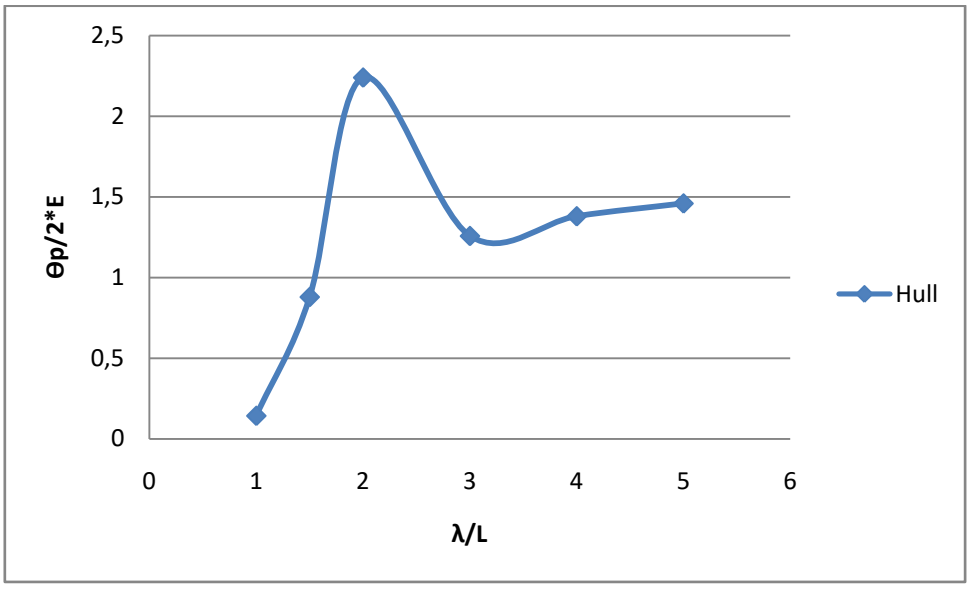

Graphic 7- Pitch RAO at 26.83 m/s, wave amplitude of 0.3 m and different wavelength/hull length relationships.

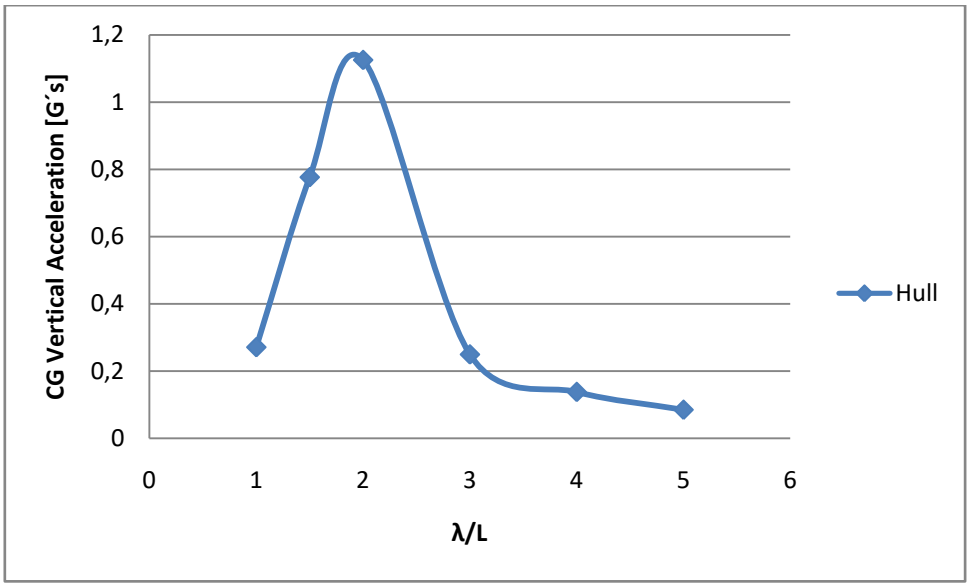

Graphic 8 - CG Vertical Acceleration RAO at 26.83 m/s, wave amplitude of 0.3 m and different wavelength/hull length relationships.

From graphics 6,7 is possible to see that at lower λ/L relationships the longitudinal oscillation, heave and pitch, amplitude responses are lesser than the wave amplitude excitation. At λ/L=2 the responses are higher than wave amplitude and they reach the maximum value, at λ/L greater than 2 the heave and pitch responses tend to follow the same wave amplitude pattern, being a little bit superior the pitch response.

From graph 8, it can be observed that at λ/L=2 the CG vertical acceleration achieves its maximum value exceeding the gravity acceleration and as far it goes to higher or lower λ/L relationships the vertical acceleration becomes to be minima and near to zero.

6.1.4 Sea State 2 Results

The simulations were done at 52.15 knots, Beam Froude Number of 4.28, that it is mean fully planing condition and with different wavelength/hull length relationships such as 1,1.5,2,3,4 and 5. The wave amplitude used to represent the sea state 2 was 0.5 meters.

A sample of the heave, pitch and vertical acceleration behavior on time is presented in graphics 9,10,11.

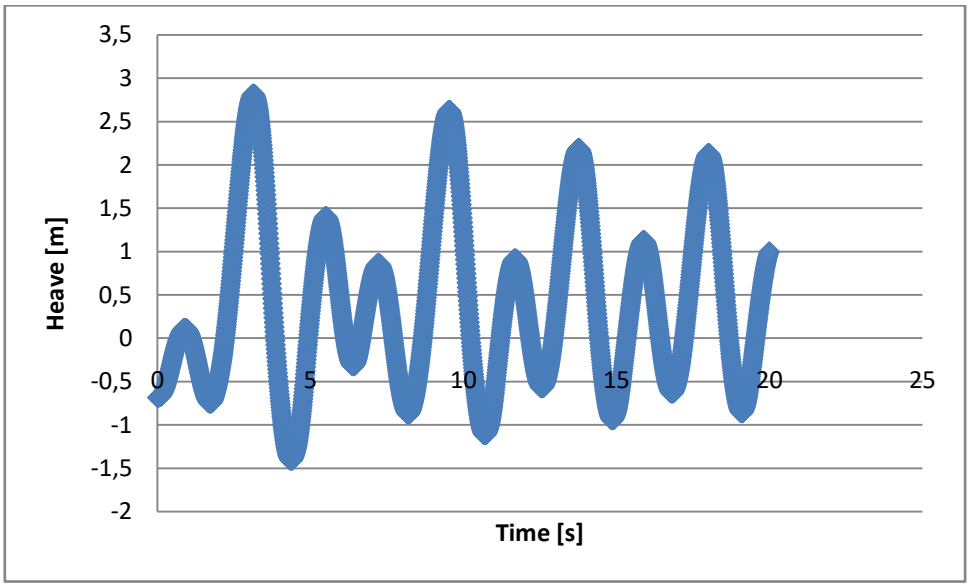

Graphic 9 - Heave Behavior in time at 26.83 m/s, wave amplitude of 0.5 m and wavelength twice the hull length.

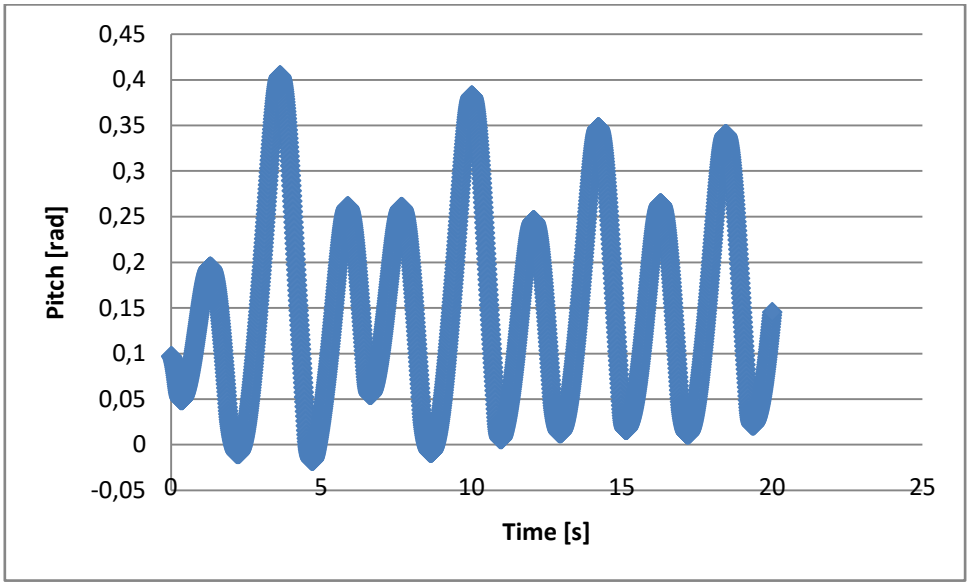

Graphic 10 - Heave Behavior in time at 26.83 m/s, wave amplitude of 0.5 m and wavelength twice the hull length.

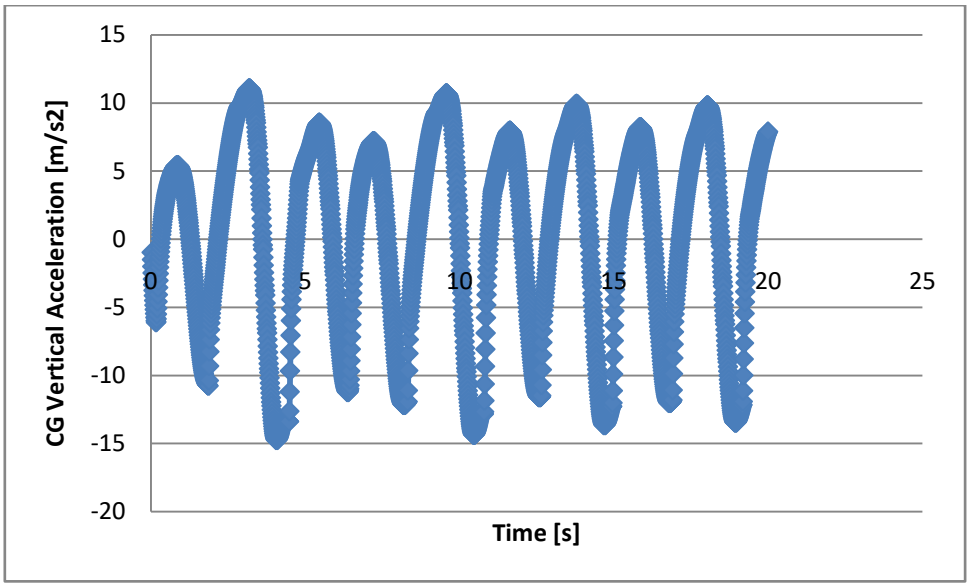

Graphic 11 - CG Vertical Acceleration Behavior in time at 26.83 m/s, wave amplitude of 0.5 m and wavelength twice the hull length.

The longitudinal pitch and heave oscillation and the vertical acceleration at CG are shown in graphics 12,13 and14. The mean run time was 20 seconds, in order to avoid noise data only the last two seconds were used. The double heave and pitch amplitudes were obtained by averaging the crest and trough values and making the difference between them, for vertical acceleration the more negative value was taken.

The doubles amplitudes were normalized by the double amplitude of the wave, for heave motion, by twice the wave slope for the pitch and by the gravity in the vertical acceleration case.

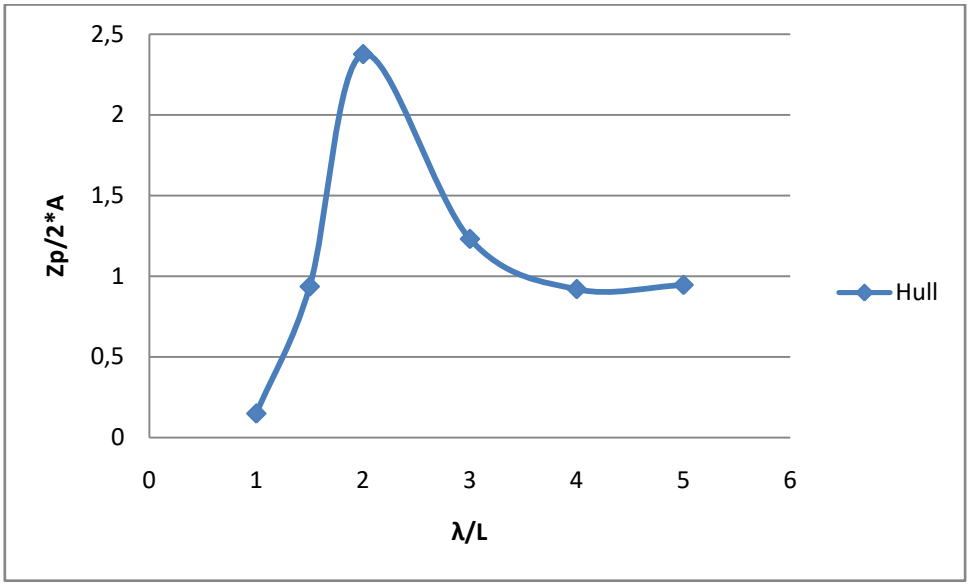

Graphic 12 - Heave RAO at 26.83 m/s, wave amplitude of 0.5 m and different wavelength/hull length relationships.

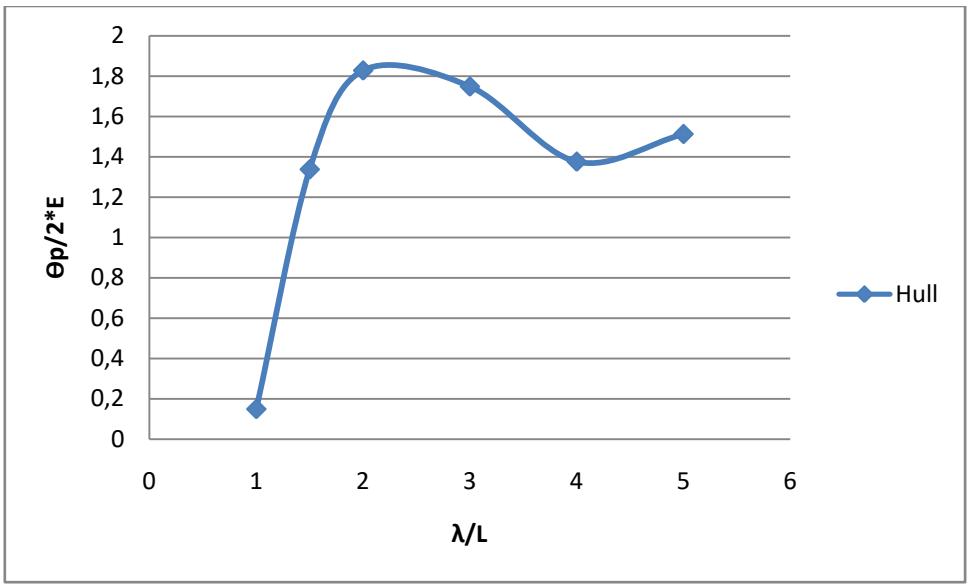

Graphic 13 - Pitch RAO at 26.83 m/s, wave amplitude of 0.5 m and different wavelength/hull length relationships.

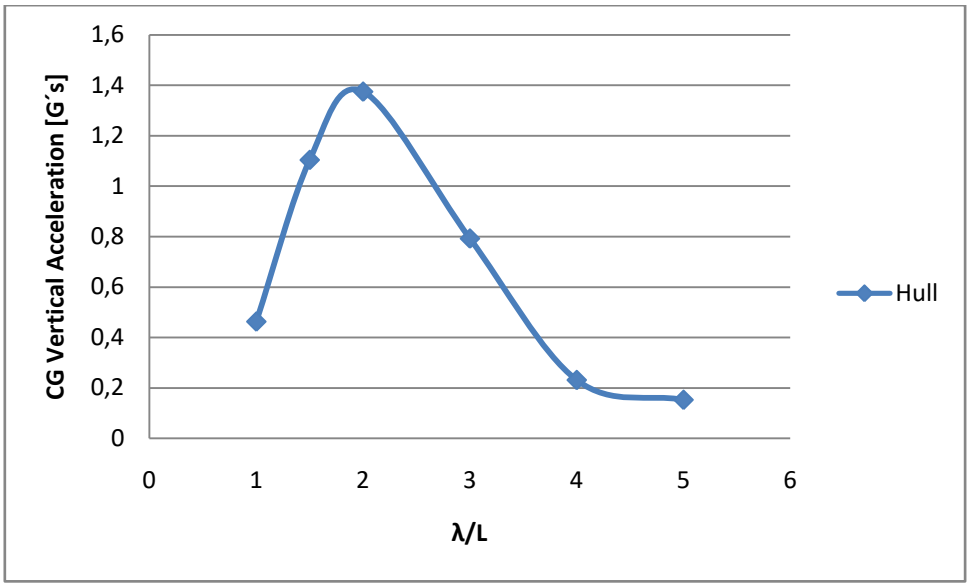

Graphic 14 - CG Vertical Acceleration RAO at 26.83 m/s, wave amplitude of 0.5 m and different wavelength/hull length relationships.

As it is appreciable in the sea state 2 results, as the wave amplitude is increased the amplitude responses both longitudinal oscillation, heave and pitch, and the vertical acceleration, increase as well, keeping the same behavior, when the wavelength/hull length is changed, as in sea state 1. Note that the pitch response still be major than the wave amplitude at λ/L greater than 2.

6.2 Hull With Hydrofoil Support

6.2.1 Assumptions Done

The assumptions contemplated here, are the same as those described in section 6.1.1

6.2.2 Mathematical Formulation Used

The mathematical model implemented are the same as in section 6.1.2 with the modification done in order to extend the model and incorporate the hydrofoil influences.
To extend the model the equation 1, which corresponds to the foil forces, was included in equations 23 and 24, which make reference to the equation of motion.

Thus the matrix system to be solve remains as,

$$\begin{bmatrix} M + M_a cos^2\theta + M_{af} & -\left(Q_a cos\theta + Q_{af}\right) \\ -\left(Q_a cos\theta + Q_{af}\right) & \left(I + I_a + I_{af}\right) \end{bmatrix} \begin{bmatrix} \ddot{Z}_{cg} \\ \ddot{\theta} \end{bmatrix} = \begin{bmatrix} F_z^* + W - F_{Zfoils}^* \\ F_\theta^* + F_{\theta foils}^* \end{bmatrix} \quad (38)$$

Where the foils added masses, momentums and added pitch mass moment of inertia are,

$$M_{af} = m_{af1} + m_{af2} \quad (39)$$

$$Q_{af} = X_{f1} \times m_{af1} + X_{f2} \times m_{af2} \quad (40)$$

$$I_{af} = X_{f1}^2 \times m_{af1} + X_{f2}^2 \times m_{af2} \quad (41)$$

And for one single foil, the forces and moments are,

$$F^*_{Zfoil} = \frac{1}{2}\rho U^2 S C_{l\alpha}(\theta_e - \theta_0) + m_{af}\dot{w}_z \qquad (42)$$

$$F^*_{\theta foil} = X_f\left\{\frac{1}{2}\rho U^2 S C_{l\alpha}(\theta_e - \theta_0) + m_{af}\dot{w}_z\right\} \qquad (43)$$

The linear system solution was done by the C++ code programmed, under the same numerical methods described in section 6.1.2.

6.2.3 Sea State 1 Results

The simulations were done at 52.15 knots, Beam Froude Number of 4.28, that it is mean fully planing condition and with different wavelength/hull length relationships such as 1,1.5,2,3,4 and 5. The wave amplitude used to represent the sea state 1 was 0.3 meters.

A sample of the heave, pitch and vertical acceleration behavior on time is presented in graphics 15,16 and 17.

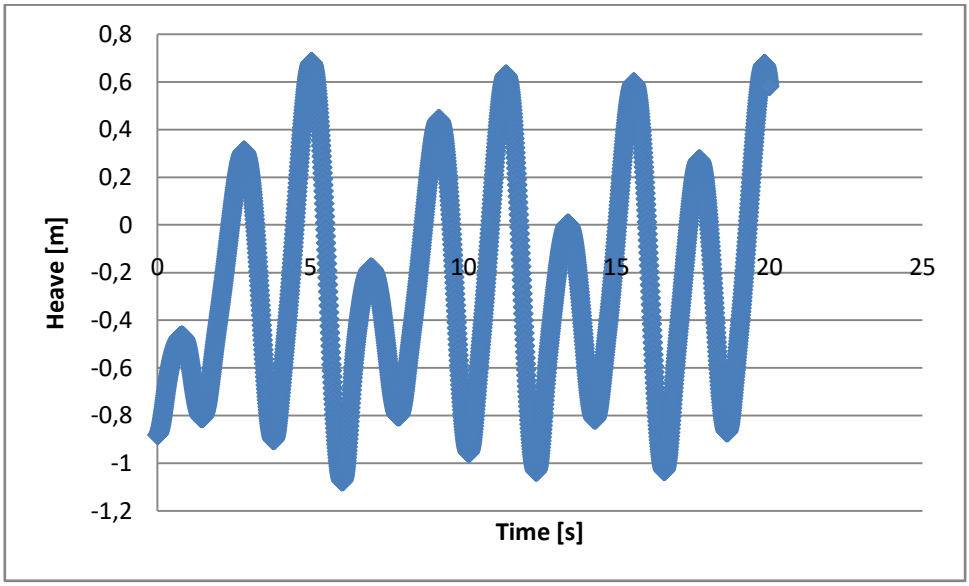

Graphic 15 - Heave Behavior in time at 26.83 m/s, wave amplitude of 0.3 m and wavelength twice the hull length.

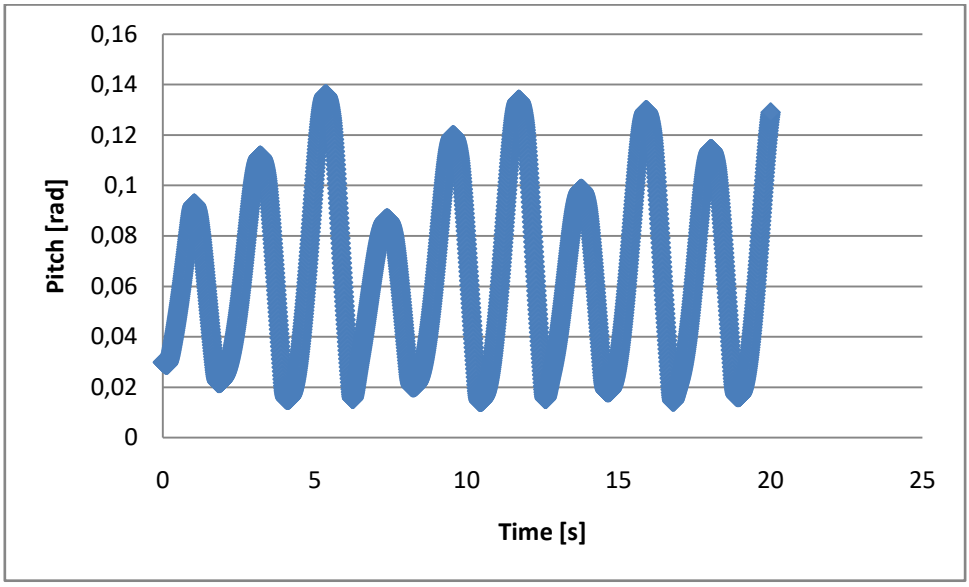

Graphic 16 - Pitch Behavior in time at 26.83 m/s, wave amplitude of 0.3 m and wavelength twice the hull length.

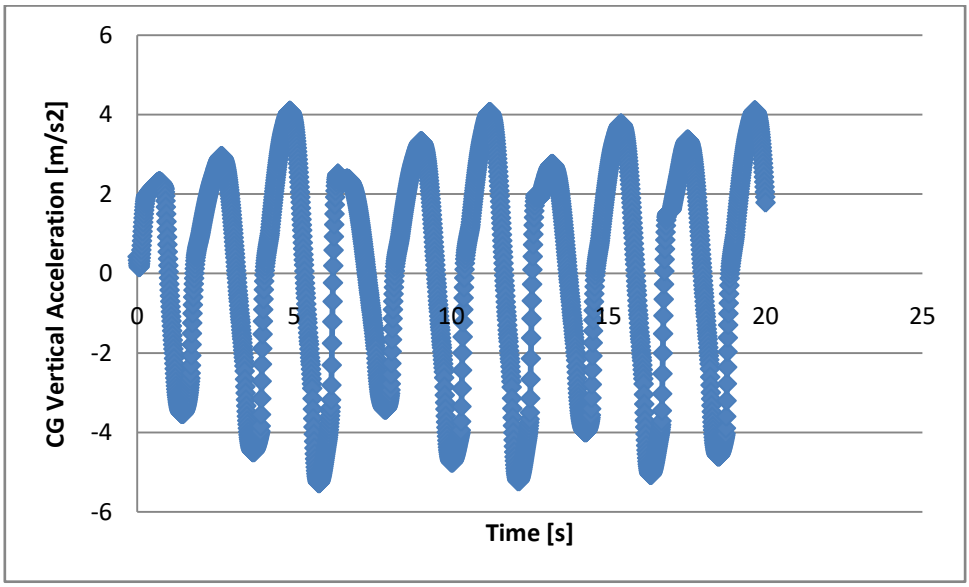

Graphic 17 - CG Vertical Acceleration Behavior in time at 26.83 m/s, wave amplitude of 0.3 m and wavelength twice the hull length.

The longitudinal pitch and heave oscillation and the vertical acceleration at CG are shown in graphics 18,19 and 20. The mean run time was 20 seconds, in order to avoid noise data only the last two seconds were used. The double heave and pitch amplitudes were obtained by averaging the crest and trough values and making the difference between them, for vertical acceleration the more negative value was taken.

The doubles amplitudes were normalized by the double amplitude of the wave, for heave motion, by twice the wave slope for the pitch and by the gravity in the vertical acceleration case.

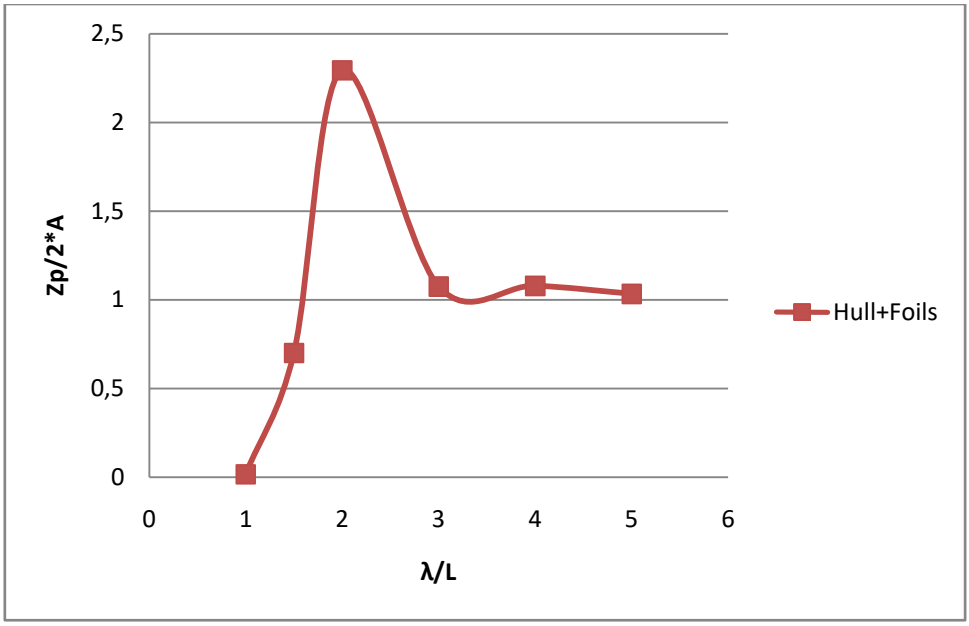

Graphic 18 - Heave RAO at 26.83 m/s, wave amplitude of 0.3 m and different wavelength/hull length relationships.

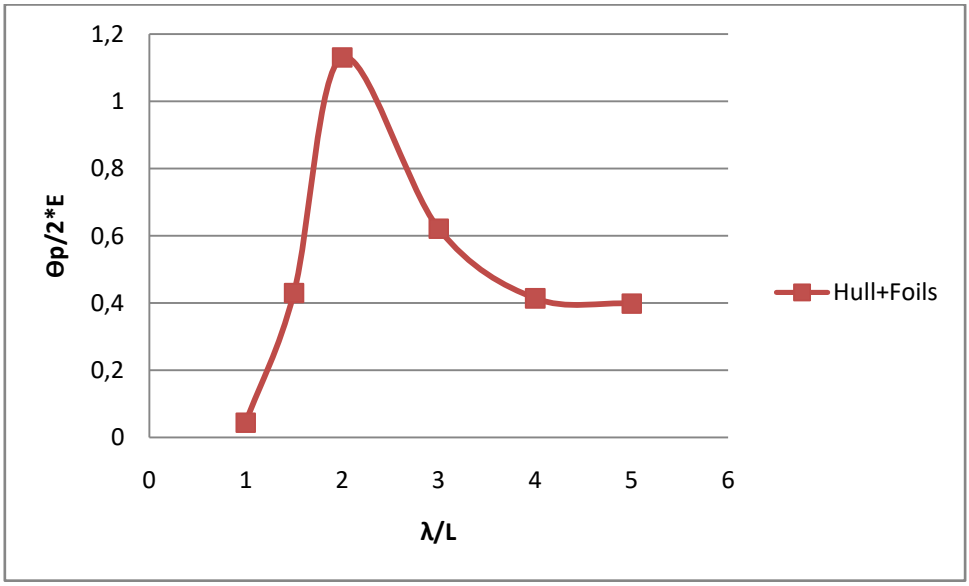

Graphic 19 - Pitch RAO at 26.83 m/s, wave amplitude of 0.3 m and different wavelength/hull length relationships.

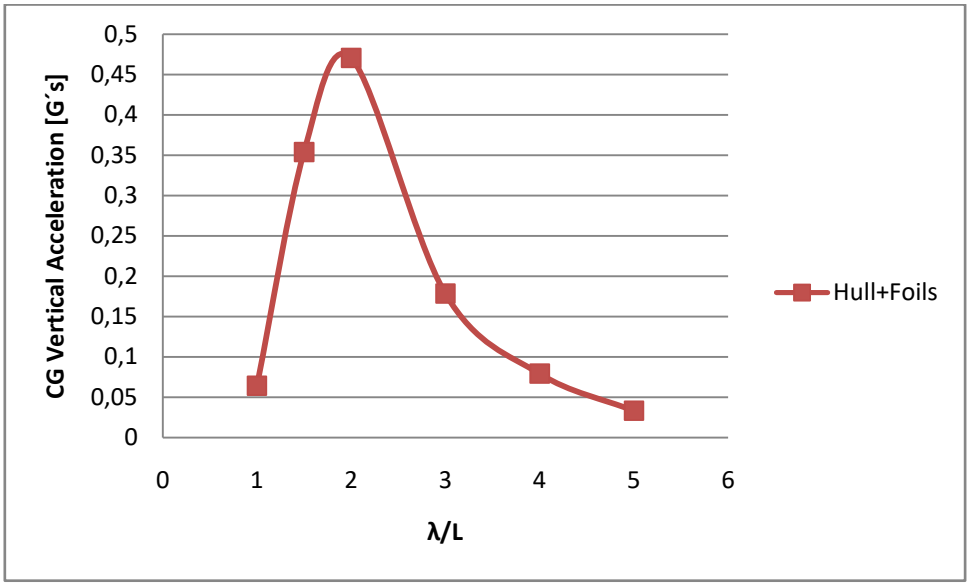

Graphic 20 - CG Vertical Acceleration RAO at 26.83 m/s, wave amplitude of 0.3 m and different wavelength/hull length relationships.

From graphics 18 and 19 is possible to see that at lower λ/L relationships the longitudinal oscillation, heave and pitch, amplitude responses are lesser than the wave amplitude excitation. At λ/L=2 the responses are higher than wave amplitude and they reach the maximum value, at λ/L greater than 2 the heave and pitch responses tend to follow the same wave amplitude pattern, being a more than twice minor the pitch response.

From graphic 20, it can be observed that at λ/L=2 the CG vertical acceleration achieves its maximum value with around half of the gravity acceleration and as far it goes to higher or lower λ/L relationships the vertical acceleration becomes to be minima and near to zero.

6.2.4 Sea State 2 Results

The simulations were done at 52.15 knots, Beam Froude Number of 4.28, that it is mean fully planing condition and with different wavelength/hull length relationships such as 1,1.5,2,3,4 and 5. The wave amplitude used to represent the sea state 2 was 0.5 meters.

A sample of the heave, pitch and vertical acceleration behavior on time is presented in graphics 21,22 and 23.

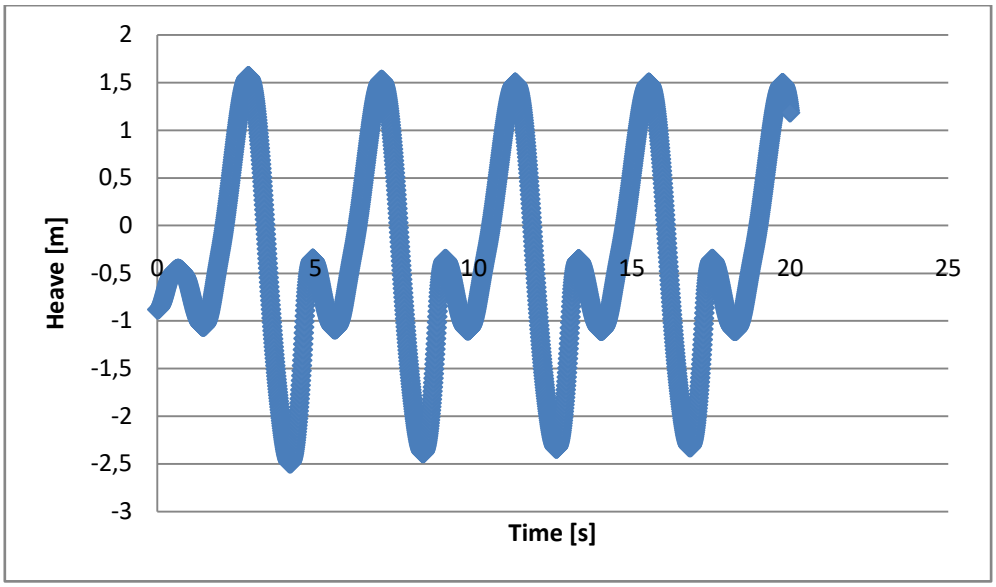

Graphic 21 - Heave Behavior in time at 26.83 m/s, wave amplitude of 0.5 m and wavelength twice the hull length.

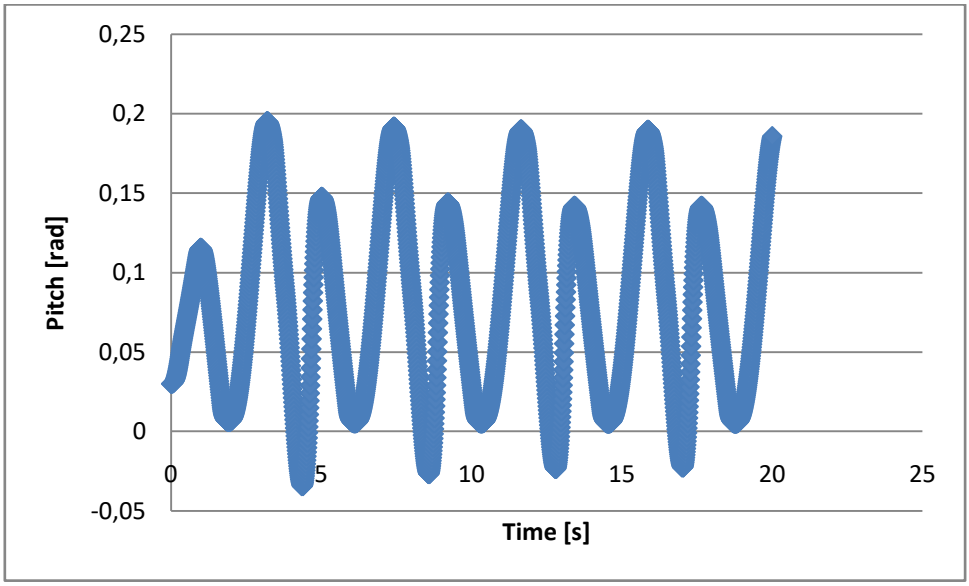

Graphic 22 - Pitch Behavior in time at 26.83 m/s, wave amplitude of 0.5 m and wavelength twice the hull length.

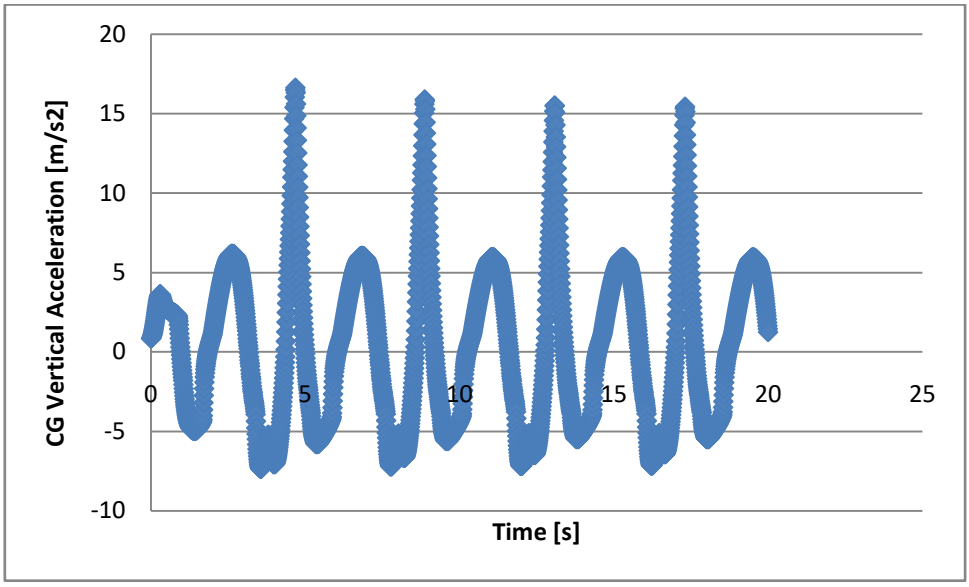

Graphic 23 - CG Vertical Acceleration Behavior in time at 26.83 m/s, wave amplitude of 0.5 m and wavelength twice the hull length.

The longitudinal pitch and heave oscillation and the vertical acceleration at CG are shown in graphics 24, 25 and 26. The mean run time was 20 seconds, in order to avoid noise data only the last two seconds were used. The double heave and pitch amplitudes were obtained by averaging the crest and trough values and making the difference between them, for vertical acceleration the more negative value was taken.

The doubles amplitudes were normalized by the double amplitude of the wave, for heave motion, by twice the wave slope for the pitch and by the gravity in the vertical acceleration case.

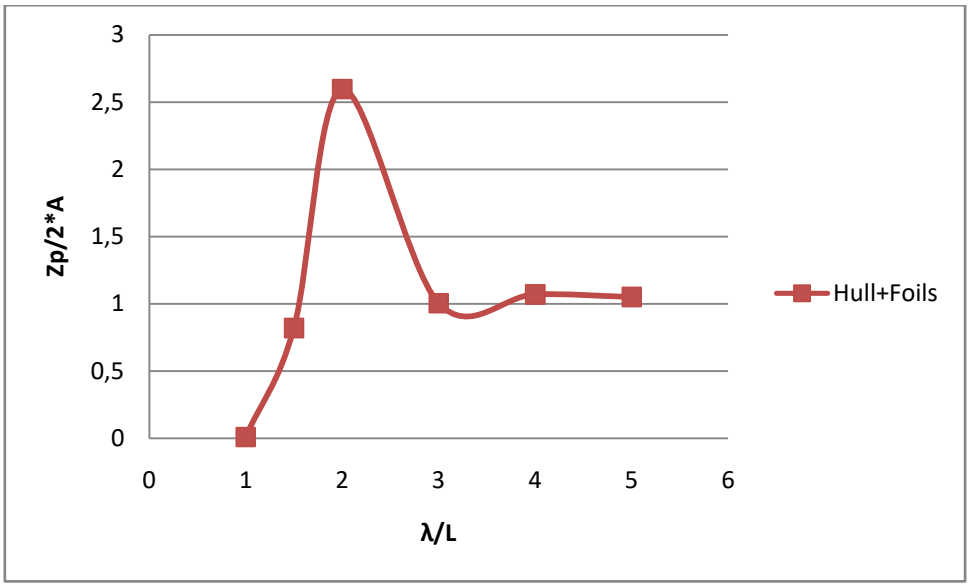

Graphic 24 - Heave RAO at 26.83 m/s, wave amplitude of 0.5 m and different wavelength/hull length relationships.

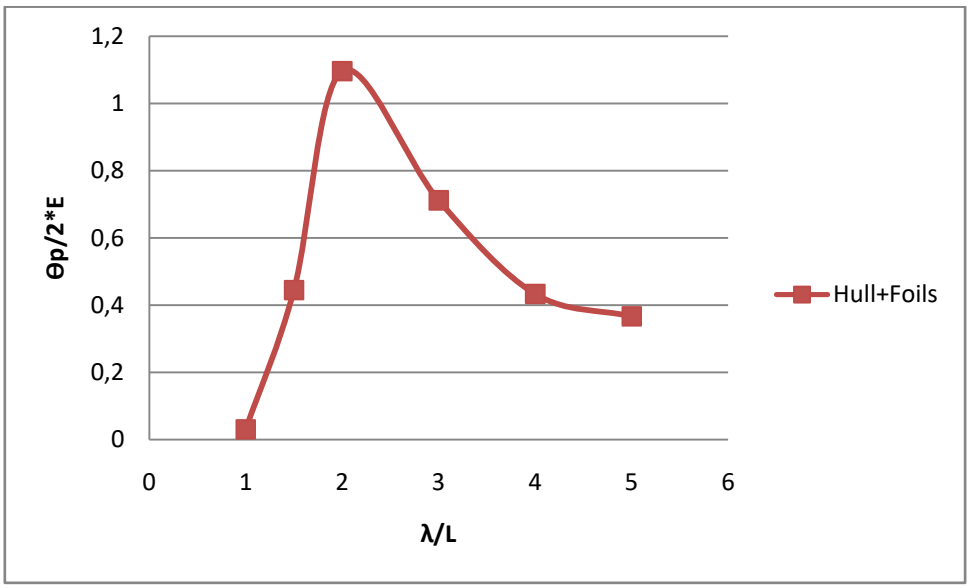

Graphic 25 - Pitch RAO at 26.83 m/s, wave amplitude of 0.5 m and different wavelength/hull length relationships.

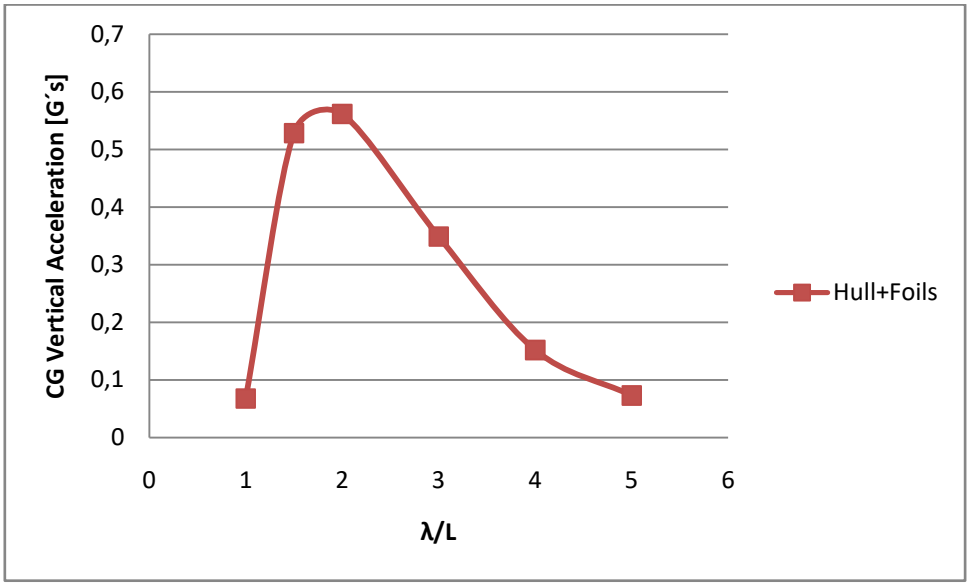

Graphic 26 - CG Vertical Acceleration RAO at 26.83 m/s, wave amplitude of 0.5 m and different wavelength/hull length relationships.

From graphics 24 and 25 is possible to see that at lower λ/L relationships the longitudinal oscillation, heave and pitch, amplitude responses are lesser than the wave amplitude excitation. At λ/L=2 the responses are higher than wave amplitude and they reach the maximum value, at λ/L greater than 2 the heave and pitch responses tend to follow the same wave amplitude pattern, being a more than twice minor the pitch response.

From graphic 20, it can be observed that at λ/L=2 the CG vertical acceleration achieves its maximum value with around half of the gravity acceleration and as far it goes to higher or lower λ/L relationships the vertical acceleration becomes to be minima and near to zero.

6.3 Comparisons

6.3.1 Sea State 1

In order to appreciate easily the differences among the results obtained with and without foils, a graphical comparison was made for both longitudinal oscillations and CG vertical acceleration. The graphics 27, 28 and 29 display the contrast of the data.

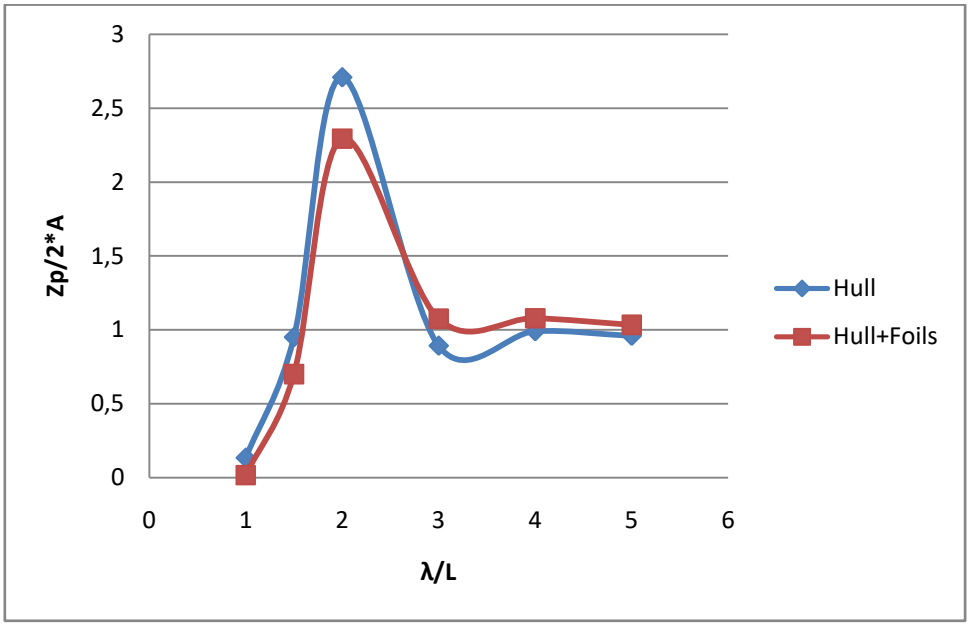

Graphic 27 - Heave RAOs comparison with/without foils at 26.83 m/s wave amplitude 0.3 m and different wavelength/hull length relationships.

In the above graphic, it can be observed that the difference among heave response amplitude with and without foils is not strong and both tend to follow the same pattern, but it is possible to says that at wavelengths lower than twice the hull length, the response is better with hydrofoil support, the reduction obtained in this stage was of 57% and the average reduction along the entire response was of 15%. At greater values of wavelength the behavior of the response was pretty similar with and without foils; This makes sense with the foil behavior in waves described in figure 7, where the response at wave motion is 100% when the hull becomes to be small in comparison with wavelength.

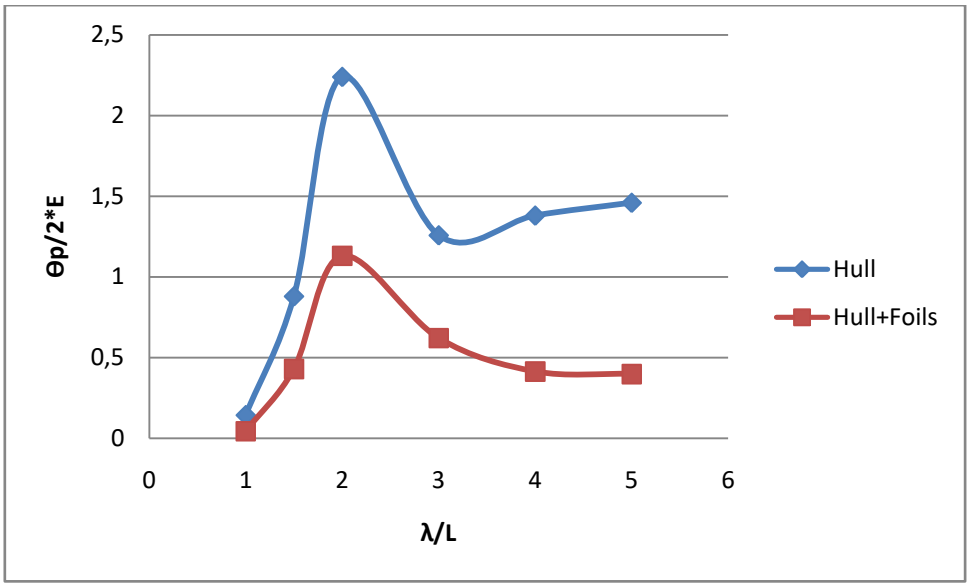

Graphic 28 - Pitch RAOs comparison with/without foils at 26.83 m/s wave amplitude 0.3 m and different wavelength/hull length relationships.

In graphic 28 the difference of the pitch response with and without foils is much more considerable, for instance at λ/L=2 the reduction of the pitch response amplitude with foils was of 49.5% and a similar tendency happen along the λ/L relationship. The average reduction of the response was of 60.5%, where the foils show a clear tendency to stabilize the pitch ship attitude.

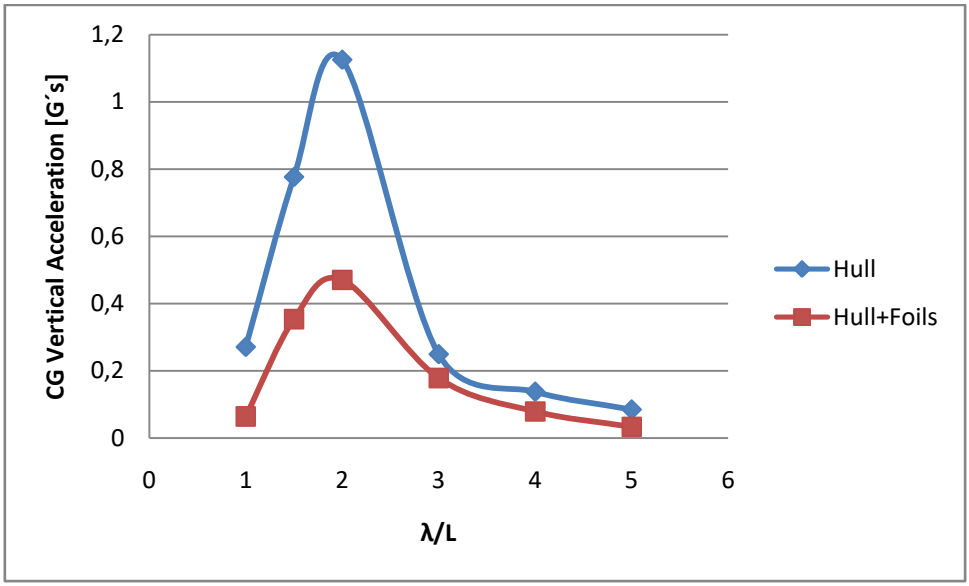

Graphic 29 - CG Vertical Acceleration RAOs comparison with/without foils at 26.83 m/s wave amplitude 0.3 m and different wavelength/hull length relationships.

About graphic 29 is possible to says that the CG vertical acceleration was strongly decreased, specially at λ/L of 1.5 and 2 where the maximum reduction achieved was of 58% and the average improvement obtained in the whole response was of 53.46%, this due to the damp in the longitudinal oscillation reached, mostly by the pitch response reduction.

6.3.2 Sea State 2

In order to appreciate easily the differences among the results obtained with and without foils, a graphical comparison was made for both longitudinal oscillations and CG vertical acceleration. The graphics 30, 31 and 32 display the contrast of the data.

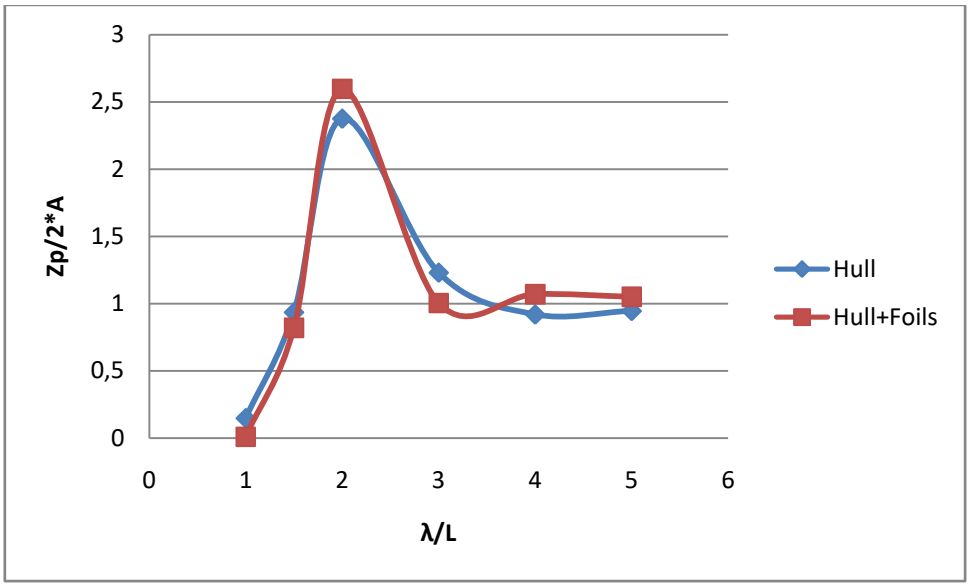

Graphic 30 - Heave RAOs comparison with/without foils at 26.83 m/s wave amplitude 0.5 m and different wavelength/hull length relationships.

In the above graphic, it can be observed that the difference among heave response amplitude with and without foils is not strong and both tend to follow the same pattern, but it is possible to says that at wavelengths lower than twice the hull length, the response is better with hydrofoil support, the reduction obtained in this stage was of 52%, that is mean 9% less than in sea state 1 and the average reduction along the entire response was of 14.5%, 3% less than sea state1. At greater values of wavelength the behavior of the response was pretty similar with and without foils; This makes sense with the foil behavior in waves described in figure 7, where the response at wave motion is 100% when the hull becomes to be small in comparison with wavelength.

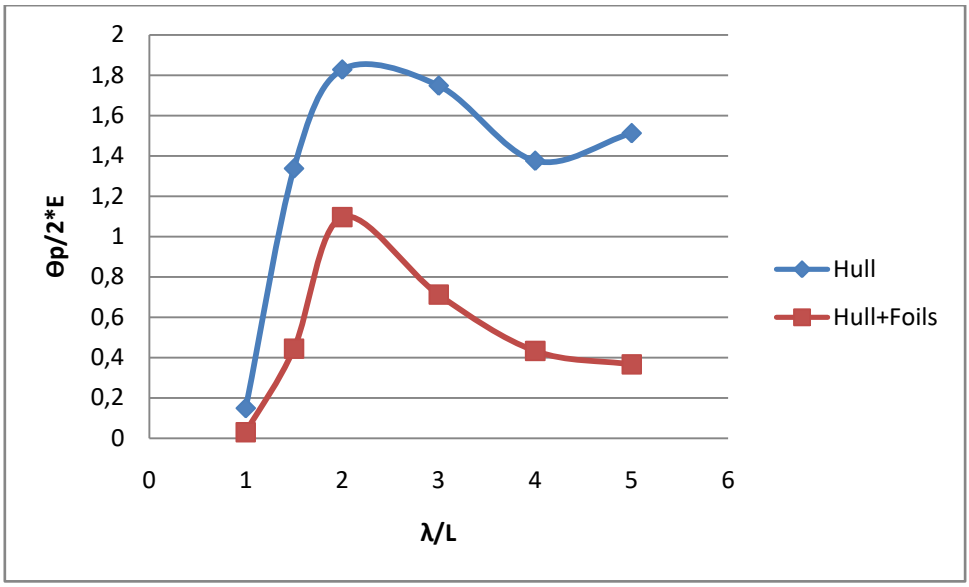

Graphic 31 - Pitch RAOs comparison with/without foils at 26.83 m/s wave amplitude 0.5 m and different wavelength/hull length relationships.

In graphic 31 the difference of the pitch response with and without foils is much more considerable, for instance at λ/L=2 the reduction of the pitch response amplitude with foils was of 39.89% and a similar tendency happen along the λ/L relationship. The amplitude reduction was around 5% less in sea state 2 than the reduction obtained at the same point in sea sate 1. The average drop of the response was of 65%, that is mean 7.7% more than sea state 1. The foils show a clear tendency to stabilize the pitch ship attitude.

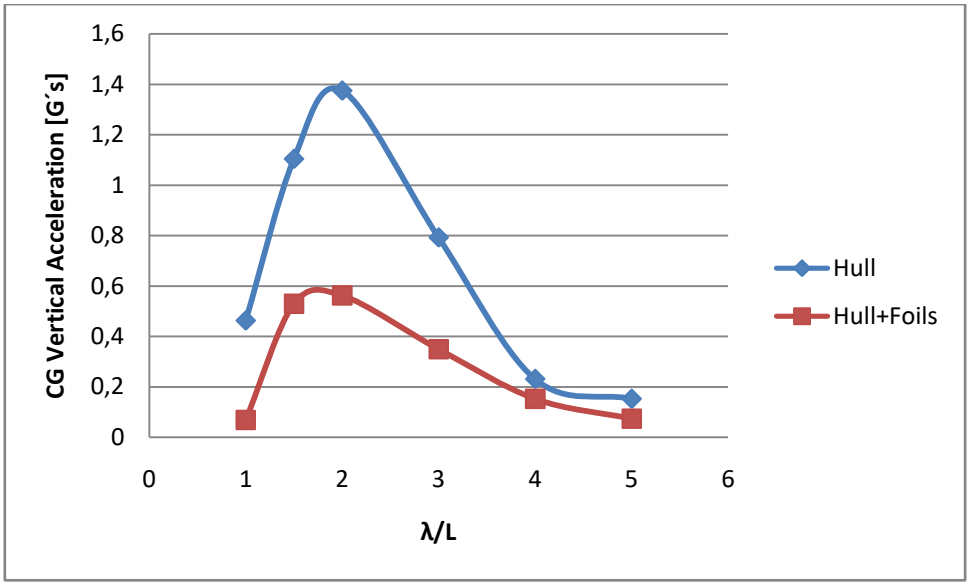

Graphic 32 - CG Vertical Acceleration RAOs comparison with/without foils at 26.83 m/s wave amplitude 0.5 m and different wavelength/hull length relationships.

About CG vertical acceleration, graphic 29, is possible to says that the CG vertical acceleration was strongly decreased, specially at λ/L of 1.5 and 2 where the reduction achieved was of 58% and the average improvement obtained in the whole response was of 65%, that represent 18.5% more than sea state 1. this due to the damp in the longitudinal oscillation reached, mostly by the greater pitch response reduction appreciated.

7. WORTH ECONOMICALLY RETROFITTING FAST CATAMARAN

To determine the feasibility to retrofit an existing catamaran, one has to take into account different parameters, such as, average operational range both velocity and sea state, the maintenance costs, the endurance of the mission profiles, position of CG, structural reinforcement, among others.

Guessing that the catamaran study object, works mostly at planinig conditions and the mainly sea states are 1 and 2, a hydrofoil assistance comparison, in calm water and seakeeping, was carried out.

The hydrofoil support was determined as 80% of the hull displacement, the foils had a rectangular fixed shape in a tandem configuration and they were located at the same level that the hull keel. For this case the following evidence were analyzed.

The total resistance of the catamaran in planing condition at calm water was reduced by 41.33%. that is means less power requirement, or less fuel consumption.

The average improvement achieved for CG vertical acceleration at both sea states was of 55%, that implies less crew affected by seasickness, longer duration of the missions under rough sea conditions, less electronic damages and better rides comfort.

That is way, under the considerations made and the evidence examined, is possible to say that the retrofit worth economically, however will be interesting extend the research, following the recommendations proposed in section 9, in order to determine a most general conclusion about the feasibility that the retrofit has, considering more study cases.

8. CONCLUSIONS

- In the case of Pitch response, the enhancement reached was easily appreciated at any wave amplitude and wavelength analyzed here, showing the tendency to stabilize the pitch ship attitude that the foils have. The average reduction obtained was 63%.

- For the Heave response, the improvement was soft in general, being more significant at lower wave amplitudes and wavelengths, the average reduction was 15% .

- With the hydrofoils support, the vertical acceleration at center of gravity CG of the catamaran was improved 55%, due to the longitudinal oscillation, heave and pitch, damp achieved, mostly by the pitch response reduction.

- At calm water, under planing condition, the performance of the catamaran was increased more than 40% due to the total resistance reduction reached.

- The improvement of seaworthiness of fast catamaran by hydrofoils support was reached, thanks to the damp of longitudinal oscillation, heave and pitch, and the vertical acceleration reduction due to the foil influence. The benefits that the hydrofoils have to damp the longitudinal motion were made evident.

- Knowing the advantages that the foils have as tool to improve the seakeeping and performance of fast catamarans, either they are a new design or a retrofits from existing one, now is possible to design hydrofoils assisted catamaran with acceptable range of accuracy and feasible retrofits procedures.

9. RECOMMENDATIONS

In order to generate a most general conclusion about the benefits that the hydrofoils support has, the following recommendation are proposed.

- Validate the result with towing tank experiments, or with RANS simulations.

- Extend the simulations range with a greater number of cases of sea states, velocities, hydrofoil shapes, configurations, foil load percentage and automatic control system also.

- Make an analysis to determine the foils to foil interaction and the foil hull interaction and its influence in the final results.

- Extend the model to incorporate the thrust and drag influence in seakeeping, as well as the added wave resistance.

- Extend the model for the general case, where the forces do not pass through the CG.

- Test different methods to predict the initial conditions of the trim and sinkage.

10. ACKNOWLEDGMENT

To University of Rostock, because all the support provided and to make this work possible.

This thesis was developed in the frame of the European Master Course in “Integrated Advanced Ship Design” named “EMSHIP” for “European Education in Advanced Ship Design”, Ref.: 159652-1-2009-1-BE-ERA MUNDUS-EMMC.

11. REFERENCES

[1] Gunther Migeotte, N. K. (2005). Design of Hydrofoil Assited Catamarans using Non Linear Vortex Lattice Method. *Journal of Marine Engineering Iranian Association of Naval Arquitecture and Marine Engineering* , 1-6,16-17.

[2] Universiteit Van Stellenbosch. (1982-1998). Hydrofoil supported water craft . *Patent No. 83/3503 - 86/2870* , 1.

[3] WELNICKI, W. (1998). The enhancement of seakeeping qualities of fast catamaran by means of stabilizing foils. *Polish Maritime Research* , 10.

[4] G. Migeottel, K. H. (n.d.). Developments in Hydrofoil Assistance for Semi-Displacement Catamarans. *Dept. of Mechanical Engineering, University of Stellenbosch* , 3-10.

[5]Toshihiko Arri, e. a. (1993). Development of a motion control system for a foil assisted catamaran Super jet 30. *Second International conference on fast sea transportation* , 2.

[6]K. Matveev, R. D. (2005) Development of the Tool for Predicting Hydrofoil System Performance and Simulating Motion of Hydrofoil-Assisted Boats. *High Speed and High Performance Ship and Craft Symposium*,1.

[7] K.G.W. Hoppe.(2001) Recent Applications of Hydrofoil-Supported Catamarans. *Fast Ferry International,* 1,2,5.

[8] R B Luhulima, et al.(2014) Selecting Monohull, Catamaran and Trimaran as Suitable Passenger Vessels Based on Stability and Seakeeping Criteria. *The 14th International Ship Stability Workshop,*1.

[9] M Kandasamy, et al.(2011) Multi-fidelity optimization of a high-speed foil-assisted semi-planing catamaran for low wake. *Journal of Marine Science and Technology, Vol. 16,* 4.

[10] WC O´Neill.(n.d) Hydrofoil ship design.18-19.

[11] Robert J. Johnston. (1985) Hydrofoils, *Naval engineers journal*, 150-151,179

[12] M Köpke. (2008) Master thesis, A passive suspension system for a hydrofoil supported catamaran. *University of Stellenbosch*, 28-29

[13] G. Migeottel, K. H. (2004) Development of modern hydrofoil assisted multi-hulls. *China International Boat Show & HPMV Conference*,6

[14] A Najafi. (2016) RANS simulation of hydrofoil effects on hydrodynamic coefficients of a planing catamaran. *Sharif University of Technology, Theran, Iran,* 1,64.

[15] Faltinsen. OM (2005) Hydrodynamics of High-Speed Marine Vehicles. *UK, Cambridge University Press.*

[16] Zarnick, E.E. (1978). *A non-linear mathematical model of motions of a planing boat in regular waves*. Technical Report. DTNSRDC-78/032, David Taylor Naval Ship Research and Development Center.

[17] Keuning, J.A. [1994]. *The non-linear behaviour of fast monohulls in head waves*. Phd Thesis, Technische Universiteit Delft.

APPENDICES

A1. Code Flow Chart

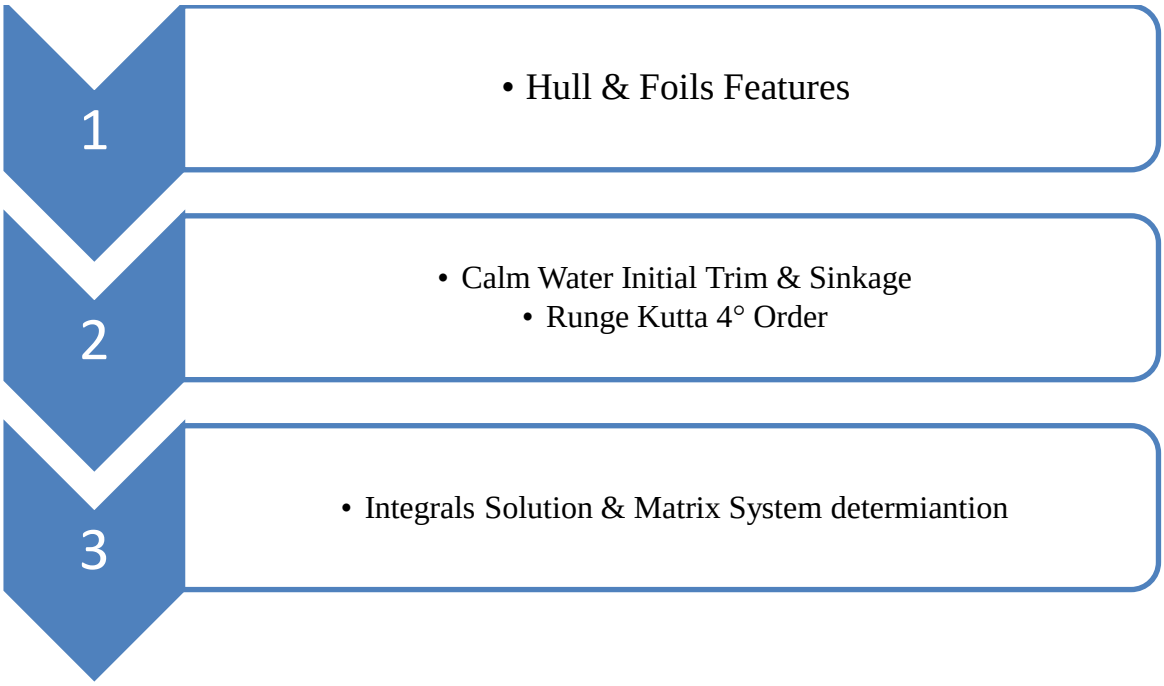

A2. C++ Code Programmed

```
#include <stdio.h>
#include <math.h>
#include <stdlib.h>
#include <iostream>
#include <fstream>

using namespace std;

//////////////////////////////
// General
//////////////////////////////

double g=9.81,                    // Gravity Acceleration [m/s^2]
      rho=1025,                  // @ 20°C, Density of sea water [kg/m^3]
      v=1e-6,                   // @ 20°C, Water Kinematic Viscosity [m2/s]
      patm=101.325,              // Atmospheric Pressure [kPa]
      pv=2.3,                   // @ 20°C, Water Vapor Pressure [kPa]
      pi=3.1416;                // Pi Number

//////////////////////////////
// Hull Features
//////////////////////////////

double M=60000,                     // Mass of the craft [kg]
      W=M*g,                       // Weight of the craft [N]
      BETA=20*(pi/180),            // Dead rise Angle [rad]
      cot=1/tan(BETA),
      lpp=20,
      LBH=4,                       // Length between Hulls [m]
      LBR=5,                       // Length - Beam Relationship
      //b0=pow(M/(4*LBR*rho*tan(BETA)),1.0/3),  // Hull Half Beam at rest [m]
      //B=2*b0,                    // Hull Beam [m]
      B=lpp/LBR,
      b0=B/2,
      d0=b0*tan(BETA),             // HUll Draft [m]
      //lpp=LBR*B,                 // Length between Perpendiculars [m]
      LCG=lpp/3,                   // CG Location [m] @ from aft
      VCG=0.3*B,                   // CG Location [m] @ from bottom
      STRN=-LCG,                   // Stern Location along the ship
      CG=0,                       // CG Location along the ship
      BOW=lpp-LCG,                 // BOW Location along the ship
      RGF=0.25,                    // Radious of Gyration, % of CG
      LSR=6,                      // Length /speed ratio
      x_dot=LSR*sqrt(lpp),         // Horizontal Velocity [m/s]
      Cv=x_dot/sqrt(g*B),          // Beam Froude number
      Cload=W/(rho*g*pow(B,3));    // Load Coefficient
      //clb=W/(0.5*rho*pow(x_dot,2)*pow(B,2));// Hull Lift coefficient with deadrise angle BETA



//////////////////////////////////////
// Foil Features (Tandem Configuration)
```

```
////////////////////////////////////

double foil_load=0.8,
     Wr=W*(1-foil_load),              // Relative weight of the ship in planing due to the foil action
     clb=Wr/(0.5*rho*pow(x_dot,2)*pow(B,2)),// Hull Lift coefficient with deadrise angle BETA
     lf=0.5*Wr,                       // Lift at  wing [N]
     Xf=LCG;                          // Arm from CG till Wing [m]

////////////////////////////////
// Wave Features
////////////////////////////////

double A=0.5,                         // Wave Amplitude [m]
     LLPR=1,                          // LAMDA /LPP ratio
     LAMDA=LLPR*lpp,                  // Wavelength [m]
     T=sqrt(LAMDA/1.56),              // Wave Period [s]
     E=(2*pi*A)/LAMDA,                // Steepness (Wave Slope)
     k=(2*pi)/LAMDA,                  // Wave Number
     Z=0,                             // Wave Orbital Velocity from it is taken
     omega=sqrt(g*k),                 // Dispersion relation
     Clamda=(lpp/LAMDA)*pow(Cload/pow(LBR,2),1.0/3);   // Wavelength Coefficient

////////////////////////////////
// Time Step
////////////////////////////////

int    N=2000;//(T*2)/0.01;           // Quantity of Intervals
double ti=0,                          // Initial Time [s]
     tf=20,//(T*2),                  // Final Time [s]
     h=(tf-ti)/N;                     // Time Step

////////////////////////////////
// Zarnick Coefficients
////////////////////////////////

double ka=1,                          // Added mass coefficient
     aBF=0.5,                         // Buoyancy correction factor
     aBM=0.5*aBF,                     // Moment correction factor
     cpu=0.5*pi,                      // Pile-up or splash up coefficient
     cd=1*cos(BETA);                  // Cross flow drag coefficient

////////////////////////////////////
// Equilibrium State
////////////////////////////////////

#define f(lamda) ((LCG/(lamda*B))-0.75+(1/(((5.21*pow(Cv,2))/pow(lamda,2))+2.39)))
#define g(lamda)
(((2*5.21*pow(Cv,2))/(pow(lamda,3)*pow(((5.21*pow(Cv,2))/pow(lamda,2))+2.39,2)))-
(LCG/(pow(lamda,2)*B)))

#define fclo(clo) (clo-(0.0065*(BETA*(180/pi))*pow(clo,0.6))-clb)
#define gclo(clo) (1-(0.6*0.0065*(BETA*(180/pi))*(1/pow(clo,0.4))))

double f_clo(double clo,double epsilon)
{
```

```
   while ((fclo(clo)*fclo(clo))>(epsilon*epsilon))
   {
      clo=clo-(fclo(clo)/gclo(clo));
   }
   return clo;
}

double lamdaW(double lamda,double epsilon)
{
   while ((f(lamda)*f(lamda))>(epsilon*epsilon))
   {
      lamda=lamda-(f(lamda)/g(lamda));
   }

   if(lamda>4)
   {
      cout<<"Lamda is: "<<lamda<<"It should be lamda <=4, please modify the hull feature at
maximum allowed"<<endl;
      exit(0);
   }

   return lamda;
}

double trim()
{
   double lamda,cl0,pitch_0,CTR;

   lamda=lamdaW(1,1e-5);
   CTR=(0.012*pow(lamda,0.5))+((0.0055*pow(lamda,2.5))/pow(Cv,2));
   cl0=f_clo(0.1,1e-5);
   pitch_0=(pi/180)*pow(cl0/CTR,1.0/1.1);

   return pitch_0;
}

double sinkage()
{
   double heave_0,pitch_0,lc,lk,xs,lamda,draft;

   lamda=lamdaW(1,1e-5);
   pitch_0=trim();
   xs=(B*tan(BETA))/(pi*tan(pitch_0));
   lc=(lamda*B)-(0.5*xs);
   lk=(2*lamda*B)-lc;
   draft=lk*sin(pitch_0);
   //cout<<draft<<endl;
   heave_0=draft+(STRN*sin(pitch_0))-(VCG*cos(pitch_0));

   return heave_0;
}

double HullDrag()
{
   double lamda,pitch_0,xs,lc,lk,drag,dragF,dragI,Re,S,cf,cf_ITTC,delta_cf,AHR;
```

```
   lamda=lamdaW(1,1e-5);
   pitch_0=trim();
   xs=(B*tan(BETA))/(pi*tan(pitch_0));
   lc=(lamda*B)-(0.5*xs);
   lk=(2*lamda*B)-lc;
   Re=(x_dot*lk)/v;
   AHR=0.00015;
   S=(((pow(tan(BETA),2))/(sin(BETA)))*(pow(B,2)/(4*pitch_0*0.5*pi)))+(lc*(B/cos(BETA)));
   cf_ITTC=0.075/pow(log10(Re)-2,2);
   delta_cf=((44*((pow(AHR/lk,1.0/3))-(10/pow(Re,1.0/3))))+0.125)/1000;
   cf=cf_ITTC+delta_cf;
   dragF=0.5*rho*pow(x_dot,2)*S*cf;
   dragI=W*pitch_0;
   drag=dragF+dragI;
   cout<<"Drag Hull: "<<drag<<endl;

   return drag;
}

double FoilSurface()
{
   double pitch_0,S,cl,FCH,sub_foil,CG_0;

   pitch_0=trim();
   CG_0=sinkage();
   sub_foil=CG_0-(0)+(VCG*cos(pitch_0));
   FCH=(sqrt((4*pow(sub_foil,2))+1))-(2*sub_foil);
   cl=(2*pi*pitch_0)*(1-(pow(FCH,2)*0.5));
   S=(2*lf)/(rho*pow(x_dot,2)*cl);

   return S;
}

double FoilDrag()
{
   double pitch_0,drag,dragF,dragI,Re,S,cf,cf_ITTC,delta_cf,AHR,C;

   S=FoilSurface();
   C=S/LBH;
   cout<<"Chord Foil: "<<C<<endl;
   Re=(x_dot*C)/v;
   AHR=0.00015;
   cf_ITTC=0.075/pow(log10(Re)-2,2);
   delta_cf=((44*((pow(AHR/C,1.0/3))-(10/pow(Re,1.0/3))))+0.125)/1000;
   cf=cf_ITTC+delta_cf;
   dragF=0.5*rho*pow(x_dot,2)*S*cf;
   dragI=lf*pitch_0;
   drag=dragF+dragI;
   cout<<"Drag Foil: "<<drag<<endl;

   return drag;
}
```

```
//////////////////////////////////////////
// Prototype Function
//////////////////////////////////////////

void motion(double, double, double, double, double, double, double&, double&);

//////////////////////////////////
// Main Function
//////////////////////////////////

int main()
{
   // Calm Water Resistance

   double H_Drag,H_Pow,Foil_Drag,Total_Pow;

   H_Drag=HullDrag();
   Foil_Drag=FoilDrag();
   H_Pow=H_Drag*x_dot;
   Total_Pow=H_Pow+(2*Foil_Drag*x_dot);

   // Initial Conditions

   double
t[N],x[N],z[N],theta[N],z_dot[N],theta_dot[N],HA[N],PA[N],SVA[N],CGVA[N],BVA[N],z_2dot,the
ta_2dot;

   t[0]=ti;

   x[0]=0+(x_dot*(ti-0));
   z[0]=sinkage();
   theta[0]=trim();            // Positions [m]

   z_dot[0]=0;
   theta_dot[0]=0;             // Velocities [m/s]

   z_2dot=0;
   theta_2dot=0;               // Acceleration [m/s2]


////////////////////////////////////
// RK4-2ODES
////////////////////////////////////

double k1z[N],k2z[N],k3z[N],k4z[N],l1z[N],l2z[N],l3z[N],l4z[N],RK_z[N],RL_z[N],

k1theta[N],k2theta[N],k3theta[N],k4theta[N],l1theta[N],l2theta[N],l3theta[N],l4theta[N],RK_theta[N]
,RL_theta[N];

double wz_str[N],wz_dot_str[N],wz_cg[N],wz_dot_cg[N],wz_bow[N],wz_dot_bow[N];

for (int i=0;i<=N;i++)
{

   // Time & Horizontal Position Update
```

```
    t[i+1]=t[i]+h;
    x[i+1]=x[i]+h*x_dot;

    motion(t[i],z_dot[i],theta_dot[i],x[i],z[i],theta[i],z_2dot,theta_2dot);
    l1z[i]=h*z_2dot;
    l1theta[i]=h*theta_2dot;

    k1z[i]=h*z_dot[i];
    k1theta[i]=h*theta_dot[i];


motion(t[i]+(h/2),z_dot[i]+(l1z[i]/2),theta_dot[i]+(l1theta[i]/2),x[i]+(0.5*h*x_dot),z[i]+(k1z[i]/2),thet
a[i]+(k1theta[i]/2),z_2dot,theta_2dot);
    l2z[i]=h*z_2dot;
    l2theta[i]=h*theta_2dot;

    k2z[i]=h*(z_dot[i]+(l1z[i]/2));
    k2theta[i]=h*(theta_dot[i]+(l1theta[i]/2));


motion(t[i]+(h/2),z_dot[i]+(l2z[i]/2),theta_dot[i]+(l2theta[i]/2),x[i]+(0.5*h*x_dot),z[i]+(k2z[i]/2),thet
a[i]+(k2theta[i]/2),z_2dot,theta_2dot);
    l3z[i]=h*z_2dot;
    l3theta[i]=h*theta_2dot;

    k3z[i]=h*(z_dot[i]+(l2z[i]/2));
    k3theta[i]=h*(theta_dot[i]+(l2theta[i]/2));


motion(t[i]+h,z_dot[i]+l3z[i],theta_dot[i]+l3theta[i],x[i]+(h*x_dot),z[i]+k3z[i],theta[i]+k3theta[i],z_2
dot,theta_2dot);
    l4z[i]=h*z_2dot;
    l4theta[i]=h*theta_2dot;

    k4z[i]=h*(z_dot[i]+l3z[i]);
    k4theta[i]=h*(theta_dot[i]+l3theta[i]);

    RL_z[i]=(l1z[i]/6)+(2*l2z[i]/6)+(2*l3z[i]/6)+(l4z[i]/6);
    RL_theta[i]=(l1theta[i]/6)+(2*l2theta[i]/6)+(2*l3theta[i]/6)+(l4theta[i]/6);

    RK_z[i]=(k1z[i]/6)+(2*k2z[i]/6)+(2*k3z[i]/6)+(k4z[i]/6);
    RK_theta[i]=(k1theta[i]/6)+(2*k2theta[i]/6)+(2*k3theta[i]/6)+(k4theta[i]/6);

    // Velocities Update
    z_dot[i+1]=z_dot[i]+RL_z[i];
    theta_dot[i+1]=theta_dot[i]+RL_theta[i];

    // Heave and Pitch Update
    z[i+1]=z[i]+RK_z[i];
    theta[i+1]=theta[i]+RK_theta[i];

    // Heave and Pitch Accelerations [m/s^2]
    HA[i]=RL_z[i];
    PA[i]=RL_theta[i];
```

```
   // Vertical Accelerations [m/s2]

   wz_str[i]=A*omega*exp(k*Z)*sin((k*(x[i]+(STRN*cos(theta[i]))+(VCG*sin(theta[i]))))-
(omega*t[i]));
   wz_dot_str[i]=-
A*pow(omega,2)*exp(k*Z)*cos((k*(x[i]+((STRN)*cos(theta[i]))+(VCG*sin(theta[i]))))-
(omega*t[i]));

   wz_cg[i]=A*omega*exp(k*Z)*sin((k*(x[i]+(CG*cos(theta[i]))+(VCG*sin(theta[i]))))-
(omega*t[i]));
   wz_dot_cg[i]=-
A*pow(omega,2)*exp(k*Z)*cos((k*(x[i]+(CG*cos(theta[i]))+(VCG*sin(theta[i]))))-(omega*t[i]));

   wz_bow[i]=A*omega*exp(k*Z)*sin((k*(x[i]+(BOW*cos(theta[i]))+(VCG*sin(theta[i]))))-
(omega*t[i]));
   wz_dot_bow[i]=-
A*pow(omega,2)*exp(k*Z)*cos((k*(x[i]+(BOW*cos(theta[i]))+(VCG*sin(theta[i]))))-(omega*t[i]));


   SVA[i]=(HA[i]*cos(theta[i]))-(PA[i]*STRN)+(theta_dot[i]*((x_dot*cos(theta[i]))-
(z_dot[i]*sin(theta[i]))))-(wz_dot_str[i]*cos(theta[i]))+(theta_dot[i]*wz_str[i]*sin(theta[i]));
   CGVA[i]=(HA[i]*cos(theta[i]))-(PA[i]*CG)+(theta_dot[i]*((x_dot*cos(theta[i]))-
(z_dot[i]*sin(theta[i]))))-(wz_dot_cg[i]*cos(theta[i]))+(theta_dot[i]*wz_cg[i]*sin(theta[i]));
   BVA[i]=(HA[i]*cos(theta[i]))-(PA[i]*BOW)+(theta_dot[i]*((x_dot*cos(theta[i]))-
(z_dot[i]*sin(theta[i]))))-(wz_dot_bow[i]*cos(theta[i]))+(theta_dot[i]*wz_bow[i]*sin(theta[i]));

}

   // Heave, Pitch & Vertical Acceleration Peaks
   double z_p,theta_p,z_pmn=0,theta_pmn,z_pmx=0,theta_pmx,SVA_p=0,CGVA_p=0,BVA_p=0;

for(int i=(N-(2/h));i<=N;i++) //Last 2 seconds of simulation (Non Disturbed Data)
{
   if(z[i]<z_pmx){z_pmx=z[i];}

   if(theta[i]>theta[0]){theta_pmx=theta[i];}
}

for(int i=(N-(2/h));i<=N;i++) //Last 2 seconds of simulation (Non Disturbed Data)
{
   if(z[i]>z_pmn){z_pmn=z[i];}

   if(theta[i]<theta[0]){theta_pmn=theta[i];}
}

for(int i=(N-(2/h));i<=N;i++)
{
   if(SVA[i]<SVA_p){SVA_p=SVA[i];}

   if(CGVA[i]<CGVA_p){CGVA_p=CGVA[i];}

   if(BVA[i]<BVA_p){BVA_p=BVA[i];}
}

  z_p=(z_pmx-z_pmn);
```

```
  theta_p=(theta_pmx-theta_pmn);

  // Heave, Pitch & Vertical Accelerations Normalized
  double z_n,theta_n,SVA_n,CGVA_n,BVA_n;

  z_n=z_p/(2*A);
  theta_n=theta_p/(2*E);
  SVA_n=SVA_p/g;
  CGVA_n=CGVA_p/g;
  BVA_n=BVA_p/g;

////////////////////////////////////////////////
// Results.txt
////////////////////////////////////////////////

  ofstream outfile;
  outfile.open("StateVector.txt");
  outfile<<"M[kg] lpp[m] B[m] LCG[m] VCG[m] d0[m] BETA[°]"<<endl;
  outfile<<M<<" "<<lpp<<" "<<2*b0<<" "<<LCG<<" "<<VCG<<" "<<d0<<"
"<<BETA*(180/pi)<<endl;
  outfile<<"A[m] E[rad] LAMDA[m] LAMDA/lpp T[s] Z_p[m] Theta_p[rad] SVA_p[m/s2]
CGVA_p[m/s2] BVA_p[m/s2] Z_n Theta_n SVA_p/g CGVA_p/g BVA_p/g "<<endl;
  outfile<<A<<" "<<E<<" "<<LAMDA<<" "<<LLPR<<" "<<T<<" "<<z_p<<"
"<<theta_p<<" "<<SVA_p<<" "<<CGVA_p<<" "<<BVA_p<<" "<<z_n<<" "<<theta_n<<"
"<<SVA_n<<" "<<CGVA_n<<" "<<BVA_n<<endl;
  outfile<<"Cv Cload Clamda TotalDrag[kN] HullPow[hp]"<<endl;
  outfile<<Cv<<" "<<Cload<<" "<<Clamda<<" "<<(H_Drag+(2*Foil_Drag))/1000<<"
"<<Total_Pow*0.00134102<<endl;
  outfile<<"Time[s] X[m] Z[m] Theta[rad] X_dot[m/s] Z_dot[m/s] Theta_dot[rad/s]
Z_2dot[m/s2] Theta_2dot[rad/s2] SVA[m/s2] CGVA[m/s2] BVA[m/s2]"<<endl;
  for(int i=0;i<=N;i++)
{
  outfile<<t[i]<<" "<<x[i]<<" "<<z[i]<<" "<<theta[i]<<" "<<x_dot<<" "<<z_dot[i]<<"
"<<theta_dot[i]<<" "<<HA[i]<<" "<<PA[i]<<" "<<SVA[i]<<" "<<CGVA[i]<<"
"<<BVA[i]<<endl;
}
  outfile.close();

return 0;
}

////////////////////////////////////
// Equation of motion
////////////////////////////////////

void motion(double t, double z_dot, double theta_dot, double x, double z, double theta, double&
z_2dot, double& theta_2dot)
{
   // Wave Features (Deep Water)

   if(E>0.25)
   {
     cout<<"The Steepness is: "<<E<<" Should be E<=0.25 "<<endl;
     exit(0);
   }
```

```
////////////////////////////////////////////////
// Foil Forces & AddedMass
////////////////////////////////////////////////

double ff1_prima,maf1,Xf1=Xf,Xf2=-
Xf,Qaf1,Iaf1,ff2_prima,maf2,Qaf2,Iaf2,C,S,Uf1,Uf2,wzf1,wzf2,wz_dotf1,wz_dotf2,FCH,theta_orbf1,
theta_orbf2,
    subf1,subf2,etaf1,etaf2,subTf1,subTf2;

S=FoilSurface();
C=S/LBH;

wzf1=A*omega*exp(k*Z)*sin((k*(x+(Xf1*cos(theta))+(VCG*sin(theta))))-(omega*t));
wz_dotf1=-A*pow(omega,2)*exp(k*Z)*cos((k*(x+(Xf1*cos(theta))+(VCG*sin(theta))))-(omega*t));
Uf1=(x_dot*cos(theta))-(sin(theta)*(z_dot-wzf1));
subf1=z-(Xf1*sin(theta))+(VCG*cos(theta));
etaf1=A*cos((k*(x+(Xf1*cos(theta))+(VCG*sin(theta))))-(omega*t));
subTf1=subf1-etaf1;

    if(subTf1<=0)
    {
       subTf1=0;
       maf1=0;
       Qaf1=maf1*Xf1;
       Iaf1=maf1*pow(Xf1,2);
       FCH=(sqrt((4*pow(subTf1,2))+1))-(2*subTf1);
       ff1_prima=(0.5*rho*pow(Uf1,2)*S*(2*pi*theta)*(1-(pow(FCH,2)*0.5)))+(maf1*wz_dotf1);
    }
    if(subTf1>0)
    {
       maf1=(pi/2)*(pow(C,2)/4)*LBH*rho;
       Qaf1=maf1*Xf1;
       Iaf1=maf1*pow(Xf1,2);
       FCH=(sqrt((4*pow(subTf1,2))+1))-(2*subTf1);
       theta_orbf1=(wzf1-(Xf1*theta_dot)-z_dot)/Uf1;
       ff1_prima=(0.5*rho*pow(Uf1,2)*S*(2*pi*(theta+theta_orbf1))*(1-
(pow(FCH,2)*0.5)))+(maf1*wz_dotf1);
    }


wzf2=A*omega*exp(k*Z)*sin((k*(x+(Xf2*cos(theta))+(VCG*sin(theta))))-(omega*t));
wz_dotf2=-A*pow(omega,2)*exp(k*Z)*cos((k*(x+(Xf2*cos(theta))+(VCG*sin(theta))))-(omega*t));
Uf2=(x_dot*cos(theta))-(sin(theta)*(z_dot-wzf2));
subf2=z-(Xf2*sin(theta))+(VCG*cos(theta));
etaf2=A*cos((k*(x+(Xf2*cos(theta))+(VCG*sin(theta))))-(omega*t));
subTf2=subTf2-etaf2;

    if(subTf2<=0)
    {
       subTf2=0;
       maf2=0;
       Qaf2=maf2*Xf2;
       Iaf2=maf2*pow(Xf2,2);
       FCH=(sqrt((4*pow(subTf2,2))+1))-(2*subTf2);
```

```
      ff2_prima=(0.5*rho*pow(Uf2,2)*S*(2*pi*theta)*(1-(pow(FCH,2)*0.5)))+(maf2*wz_dotf2);
    }
    if(subTf2>0)
    {
      maf2=(pi/2)*(pow(C,2)/4)*LBH*rho;
      Qaf2=maf2*Xf2;
      Iaf2=maf2*pow(Xf2,2);
      FCH=(sqrt((4*pow(subTf2,2))+1))-(2*subTf2);
      theta_orbf2=(wzf2-(Xf2*theta_dot)-z_dot)/Uf2;
      ff2_prima=(0.5*rho*pow(Uf2,2)*S*(2*pi*(theta+theta_orbf2))*(1-
(pow(FCH,2)*0.5)))+(maf2*wz_dotf2);
    }



////////////////////////////////////////////////
// Forces & Mass Inertia Computation
////////////////////////////////////////////////

// Hull Forces
// Trapezoidal Method - Integrals solution

   int n=21;
   double
p0[n],p_i[n],U0[n],Ui[n],V0[n],Vi[n],eta0[n],etai[n],eta0_dot[n],etai_dot[n],sub0[n],subi[n],d_0[n],di[
n],dse0[n],dsei[n],b_0[n],bi[n],

ma0[n],mai[n],b0_dot[n],bi_dot[n],ma0_dot[n],mai_dot[n],wz0[n],wzi[n],wz0_dot[n],wzi_dot[n],wz0
_s[n],wzi_s[n],delta;

   delta=(lpp-0)/n;

for (int i=0;i<=n;i++)
{
   p0[i]=0+(i*delta);
   p_i[i]=0+((i+1)*delta);

   wz0[i]=A*omega*exp(k*Z)*sin((k*(x+(p0[i]*cos(theta))+(VCG*sin(theta))))-(omega*t));
   wzi[i]=A*omega*exp(k*Z)*sin((k*(x+(p_i[i]*cos(theta))+(VCG*sin(theta))))-(omega*t));

   wz0_dot[i]=-A*pow(omega,2)*exp(k*Z)*cos((k*(x+(p0[i]*cos(theta))+(VCG*sin(theta))))-
(omega*t));
   wzi_dot[i]=-A*pow(omega,2)*exp(k*Z)*cos((k*(x+(p_i[i]*cos(theta))+(VCG*sin(theta))))-
(omega*t));

   wz0_s[i]=k*cos(theta)*A*omega*exp(k*Z)*cos((k*(x+(p0[i]*cos(theta))+(VCG*sin(theta))))-
(omega*t));
   wzi_s[i]=k*cos(theta)*A*omega*exp(k*Z)*cos((k*(x+(p_i[i]*cos(theta))+(VCG*sin(theta))))-
(omega*t));

   U0[i]=(x_dot*cos(theta))-(sin(theta)*(z_dot-wz0[i]));
   Ui[i]=(x_dot*cos(theta))-(sin(theta)*(z_dot-wzi[i]));

   V0[i]=(x_dot*sin(theta))-(theta_dot*p0[i])+(cos(theta)*(z_dot-wz0[i]));
   Vi[i]=(x_dot*sin(theta))-(theta_dot*p_i[i])+(cos(theta)*(z_dot-wzi[i]));
```

```
   d_0[i]=z-(p0[i]*sin(theta))+(VCG*cos(theta));
   di[i]=z-(p_i[i]*sin(theta))+(VCG*cos(theta));

   eta0[i]=A*cos((k*(x+(p0[i]*cos(theta))+(VCG*sin(theta))))-(omega*t));
   etai[i]=A*cos((k*(x+(p_i[i]*cos(theta))+(VCG*sin(theta))))-(omega*t));

   eta0_dot[i]=A*omega*sin((k*(x+(p0[i]*cos(theta))+(VCG*sin(theta))))-(omega*t));
   etai_dot[i]=A*omega*sin((k*(x+(p_i[i]*cos(theta))+(VCG*sin(theta))))-(omega*t));

   sub0[i]=d_0[i]-eta0[i];
   subi[i]=di[i]-etai[i];

if(sub0[i]<=0)
   {
     b_0[i]=0;
     ma0[i]=0;
     b0_dot[i]=0;
     ma0_dot[i]=0;
   }
if(subi[i]<=0)
   {
     bi[i]=0;
     mai[i]=0;
     bi_dot[i]=0;
     mai_dot[i]=0;
   }

if(sub0[i]>0)
   {
    dse0[i]=sub0[i]/(cos(theta)-(eta0_dot[i]*sin(theta)));
    if(dse0[i]>=d0*(2/pi))
    {
      b_0[i]=b0;
      ma0[i]=ka*pi*0.5*rho*pow(b_0[i],2);
      b0_dot[i]=0;
      ma0_dot[i]=0;
    }
    if(dse0[i]<d0*(2/pi))
    {
       b_0[i]=dse0[i]*cpu*cot;
       ma0[i]=ka*pi*0.5*rho*pow(b_0[i],2);
       b0_dot[i]=(z_dot-eta0_dot[i])/(cos(theta)-(eta0_dot[i]*sin(theta)));
       ma0_dot[i]=ka*pi*rho*b_0[i]*cpu*cot*b0_dot[i];
    }
   }

if(subi[i]>0)
   {
    dsei[i]=subi[i]/(cos(theta)-(etai_dot[i]*sin(theta)));
    if(dsei[i]>=d0*(2/pi))
    {
      bi[i]=b0;
      mai[i]=ka*pi*0.5*rho*pow(bi[i],2);
      bi_dot[i]=0;
```

```
      mai_dot[i]=0;
    }
    if(dsei[i]<d0*(2/pi))
    {
       bi[i]=dsei[i]*cpu*cot;
       mai[i]=ka*pi*0.5*rho*pow(bi[i],2);
       bi_dot[i]=(z_dot-etai_dot[i])/(cos(theta)-(etai_dot[i]*sin(theta)));
       mai_dot[i]=ka*pi*rho*bi[i]*cpu*cot*bi_dot[i];
    }
   }

}

double
Ma,Qa,Ia,f1z,f2z,f3z,f4z,f5z,f6z,f7z,f8z,f9z,f_z_prima,f1o,f2o,f3o,f4o,f5o,f6o,f7o,f8o,f9o,f10o,f_thet
a_prima;

//////////////////////////////////////////
// Hull AddedMass Inertia
//////////////////////////////////////////

// Hull Mass - Inertia

double I;
I=M*pow(RGF*lpp,2);                  // Ship Mass Inertia [kg*m4]

double yma[n],sum_yma=0;
for(int i=0;i<=n;i++)
{
   yma[i]=(ma0[i]+mai[i])/2;
   sum_yma=sum_yma+yma[i];
}
   Ma=sum_yma*delta;


double yqa[n],sum_yqa=0;
for(int i=0;i<=n;i++)
{
   yqa[i]=((ma0[i]*p0[i])+(mai[i]*p_i[i]))/2;
   sum_yqa=sum_yqa+yqa[i];
}
   Qa=sum_yqa*delta;

double yIa[n],sum_yIa=0;
for(int i=0;i<=n;i++)
{
   yIa[i]=((ma0[i]*pow(p0[i],2))+(mai[i]*pow(p_i[i],2)))/2;
   sum_yIa=sum_yIa+yIa[i];
}
   Ia=sum_yIa*delta;

//////////////////////////////////////////////
// Heave Force Fz
//////////////////////////////////////////////
```

```
double yf1z[n],sum_f1z=0;
for (int i=0;i<=n;i++)
   {
   yf1z[i]=((ma0[i]*(wz0_dot[i]-(U0[i]*wz0_s[i]))*pow(cos(theta),2))+(mai[i]*(wzi_dot[i]-
(Ui[i]*wzi_s[i]))*pow(cos(theta),2)))/2;
   sum_f1z=sum_f1z+yf1z[i];
   }

   f1z=sum_f1z*delta;

double yf2z[n],sum_f2z=0;
for (int i=0;i<=n;i++)
   {
   yf2z[i]=((ma0[i]*U0[i]*wz0_s[i]*pow(cos(theta),2))+(mai[i]*Ui[i]*wzi_s[i]*pow(cos(theta),2)))/2;
   sum_f2z=sum_f2z+yf2z[i];
   }

   f2z=sum_f2z*delta;

   f3z=cos(theta)*Ma*theta_dot*((z_dot*sin(theta))-(x_dot*cos(theta)));

double yf4z[n],sum_f4z=0;
for (int i=0;i<=n;i++)
   {

yf4z[i]=((ma0[i]*wz0[i]*theta_dot*sin(theta)*cos(theta))+(mai[i]*wzi[i]*theta_dot*sin(theta)*cos(the
ta)))/2;
   sum_f4z=sum_f4z+yf4z[i];
   }

   f4z=sum_f4z*delta;

double yf5z[n],sum_f5z=0;
for (int i=0;i<=n;i++)
   {
   yf5z[i]=((V0[i]*ma0_dot[i]*cos(theta))+(Vi[i]*mai_dot[i]*cos(theta)))/2;
   sum_f5z=sum_f5z+yf5z[i];
   }

   f5z=sum_f5z*delta;

double wz_STR,U,V,d,dse,bse,eta,eta_dot,sub,ma;
     wz_STR=A*omega*exp(k*Z)*sin((k*(x+(STRN*cos(theta))+(VCG*sin(theta))))-(omega*t));;
     U=(x_dot*cos(theta))-(sin(theta)*(z_dot-wz_STR));
     V=(x_dot*sin(theta))-(theta_dot*(STRN))+(cos(theta)*(z_dot-wz_STR));
     d=z-(STRN*sin(theta))+(VCG*cos(theta));
     eta=A*cos((k*(x+(STRN*cos(theta))+(VCG*sin(theta))))-(omega*t));
     eta_dot=A*omega*sin((k*(x+(STRN*cos(theta))+(VCG*sin(theta))))-(omega*t));
     sub=d-eta;

     if(sub<=0)
     {
        bse=0;
        ma=ka*pi*0.5*rho*pow(bse,2);
     }
```

```
      if(sub>0)
      {
         dse=sub/(cos(theta)-(eta_dot*sin(theta)));
         if(dse>=d0*(2/pi))
         {
            bse=b0;
            ma=ka*pi*0.5*rho*pow(bse,2);
         }
         if(dse<d0*(2/pi))
         {
            bse=cpu*dse*cot;
            ma=ka*pi*0.5*rho*pow(bse,2);
         }
      }

      f6z=U*V*ma*cos(theta);

double yf7z[n],sum_f7z=0;

for (int i=0;i<=n;i++)
   {

yf7z[i]=((ma0[i]*V0[i]*wz0_s[i]*sin(theta)*cos(theta))+(mai[i]*Vi[i]*wzi_s[i]*sin(theta)*cos(theta))
)/2;
   sum_f7z=sum_f7z+yf7z[i];
   }

   f7z=sum_f7z*delta;

double yf8z[n],sum_f8z=0;

for (int i=0;i<=n;i++)
   {
   yf8z[i]=((cd*rho*b_0[i]*pow(V0[i],2)*cos(theta))+(cd*rho*bi[i]*pow(Vi[i],2)*cos(theta)))/2;
   sum_f8z=sum_f8z+yf8z[i];
   }

   f8z=sum_f8z*delta;

double yf9z[n],sum_f9z=0;
for (int i=0;i<=n;i++)
   {
   yf9z[i]=((aBF*rho*g*(2*b_0[i]*(sub0[i]-(0.5*b_0[i]))))+(aBF*rho*g*(2*bi[i]*(subi[i]-
(0.5*bi[i])))))/2;
   sum_f9z=sum_f9z+yf9z[i];
   }

   f9z=sum_f9z*delta;

   // F_z_Prime
   f_z_prima=f1z+f2z+f3z-f4z-f5z-f6z-f7z-f8z+f9z;


//////////////////////////////////////////
// Pitch Force F_theta
```

```
//////////////////////////////////////////


double yf1o[n],sum_f1o=0;
for (int i=0;i<=n;i++)
   {
   yf1o[i]=((ma0[i]*(wz0_dot[i]-(U0[i]*wz0_s[i]))*p0[i]*cos(theta))+(mai[i]*(wzi_dot[i]-
(Ui[i]*wzi_s[i]))*p_i[i]*cos(theta)))/2;
   sum_f1o=sum_f1o+yf1o[i];
   }

   f1o=sum_f1o*delta;

double yf2o[n],sum_f2o=0;
for (int i=0;i<=n;i++)
   {
   yf2o[i]=((ma0[i]*U0[i]*wz0_s[i]*p0[i]*cos(theta))+(mai[i]*Ui[i]*wzi_s[i]*p_i[i]*cos(theta)))/2;
   sum_f2o=sum_f2o+yf2o[i];
   }

   f2o=sum_f2o*delta;

   f3o=Qa*theta_dot*((z_dot*sin(theta))-(x_dot*cos(theta)));

double yf4o[n],sum_f4o=0;
for (int i=0;i<=n;i++)
   {
   yf4o[i]=((ma0[i]*wz0[i]*theta_dot*sin(theta)*p0[i])+(mai[i]*wzi[i]*theta_dot*sin(theta)*p_i[i]))/2;
   sum_f4o=sum_f4o+yf4o[i];
   }

   f4o=sum_f4o*delta;

double yf5o[n],sum_f5o=0;
for (int i=0;i<=n;i++)
   {
   yf5o[i]=((V0[i]*ma0_dot[i]*p0[i])+(Vi[i]*mai_dot[i]*p_i[i]))/2;
   sum_f5o=sum_f5o+yf5o[i];
   }

   f5o=sum_f5o*delta;

double yf6o[n],sum_f6o=0;
for (int i=0;i<=n;i++)
   {
   yf6o[i]=((cd*rho*b_0[i]*pow(V0[i],2)*p0[i])+(cd*rho*bi[i]*pow(Vi[i],2)*p_i[i]))/2;
   sum_f6o=sum_f6o+yf6o[i];
   }

   f6o=sum_f6o*delta;

double yf7o[n],sum_f7o=0;
for (int i=0;i<=n;i++)
   {
```

```
   yf7o[i]=((aBM*rho*g*(2*b_0[i]*(sub0[i]-
(0.5*b_0[i])))*cos(theta)*p0[i])+(aBM*rho*g*(2*bi[i]*(subi[i]-(0.5*bi[i])))*cos(theta)*p_i[i]))/2;
   sum_f7o=sum_f7o+yf7o[i];
   }

   f7o=sum_f7o*delta;

   f8o=U*V*ma*STRN;

double yf9o[n],sum_f9o=0;
for (int i=0;i<=n;i++)
   {
   yf9o[i]=((ma0[i]*U0[i]*V0[i])+(mai[i]*Ui[i]*Vi[i]))/2;
   sum_f9o=sum_f9o+yf9o[i];
   }

    f9o=sum_f9o*delta;

double yf10o[n],sum_f10o=0;
for (int i=0;i<=n;i++)
   {
   yf10o[i]=((ma0[i]*V0[i]*wz0_s[i]*p0[i]*sin(theta))+(mai[i]*Vi[i]*wzi_s[i]*p_i[i]*sin(theta)))/2;
   sum_f10o=sum_f10o+yf10o[i];
   }

    f10o=sum_f10o*delta;

   // Ftheta
   f_theta_prima=-f1o-f2o-f3o+f4o+f5o+f6o+f7o+f8o+f9o+f10o;


////////////////////////////////////////
// Matrix System
////////////////////////////////////////

double A00,A01,A10,A11,Bm0,Bm1;

  //  Matrix Mass Inertia, A
      A00=M+Ma*pow(cos(theta),2)+maf1+maf2;
      A01=-(Qa*cos(theta)+Qaf1+Qaf2);
      A10=-(Qa*cos(theta)+Qaf1+Qaf2);
      A11=I+Ia+Iaf1+Iaf2;

       // Forces Vector
      Bm0=f_z_prima+W-ff1_prima-ff2_prima;
      Bm1=f_theta_prima+(ff1_prima*Xf)-(ff2_prima*Xf);

  //  Vertical Accelerations
      z_2dot=((Bm0*A11)-(Bm1*A01))/((A00*A11)-(A10*A01));
      theta_2dot=((Bm1*A00)-(Bm0*A10))/((A00*A11)-(A10*A01));

}
```